Simplified models for dark matter searches at the LHC

Abdallah, J.; et al., [Unknown]; De Jong, P.; Liem, S.; McCabe, C.; Pani, P.; Salek, D.; Tunnell, C.

DOI
10.1016/j.dark.2015.08.001

Publication date
2015

Document Version
Final published version

Published in
Physics of the Dark Universe

Physics of the Dark Universe 9–10 (2015) 8–23

Contents lists available at ScienceDirect

Physics of the Dark Universe

journal homepage: www.elsevier.com/locate/dark

Simplified models for dark matter searches at the LHC

Jalal Abdallah [1,†], Henrique Araujo [2], Alexandre Arbey [3,4,5], Adi Ashkenazi [6], Alexander Belyaev [7], Joshua Berger [8], Celine Boehm [9], Antonio Boveia [5], Amelia Brennan [10], Jim Brooke [11], Oliver Buchmueller [2], Matthew Buckley [12,†], Giorgio Busoni [13,†], Lorenzo Calibbi [14,15,†], Sushil Chauhan [16], Nadir Daci [17], Gavin Davies [2], Isabelle De Bruyn [17], Paul De Jong [18], Albert De Roeck [5], Kees de Vries [2], Daniele Del Re [19], Andrea De Simone [13], Andrea Di Simone [20], Caterina Doglioni [21], Matthew Dolan [8], Herbi K. Dreiner [22], John Ellis [5,23], Sarah Eno [24], Erez Etzion [6], Malcolm Fairbairn [23], Brian Feldstein [25], Henning Flaecher [11], Eric Feng [26], Patrick Fox [27], Marie-Hélène Genest [28], Loukas Gouskos [29], Johanna Gramling [21], Ulrich Haisch [5,25,†], Roni Harnik [27], Anthony Hibbs [25], Siewyan Hoh [30], Walter Hopkins [31], Valerio Ippolito [32], Thomas Jacques [21], Felix Kahlhoefer [33,†], Valentin V. Khoze [9], Russell Kirk [34,†], Andreas Korn [35], Khristian Kotov [36], Shuichi Kunori [37], Greg Landsberg [38], Sebastian Liem [39], Tongyan Lin [40,41,†], Steven Lowette [17], Robyn Lucas [2,42], Luca Malgeri [5], Sarah Malik [2], Christopher McCabe [9,39], Alaettin Serhan Mete [43], Enrico Morgante [21,†], Stephen Mrenna [27], Yu Nakahama [5,44], Dave Newbold [11], Karl Nordstrom [45], Priscilla Pani [18], Michele Papucci [46,47], Sophio Pataraia [48], Bjoern Penning [40], Deborah Pinna [49], Giacomo Polesello [50], Davide Racco [21], Emanuele Re [25], Antonio Walter Riotto [21], Thomas Rizzo [8], David Salek [18,39], Subir Sarkar [25], Steven Schramm [51], Patrick Skubic [52], Oren Slone [6], Juri Smirnov [53,†], Yotam Soreq [54], Timothy Sumner [2], Tim M.P. Tait [43,†], Marc Thomas [7,42], Ian Tomalin [42], Christopher Tunnell [18], Alessandro Vichi [5], Tomer Volansky [6], Neal Weiner [55], Stephen M. West [34], Monika Wielers [42], Steven Worm [42,*,†], Itay Yavin [56,57], Bryan Zaldivar [15], Ning Zhou [43], Kathryn Zurek [46,47]

[1] *Academia Sinica Institute of Physics, Taipei 11529, Taiwan*
[2] *Imperial College London High Energy Physics, London SW7 2AZ, United Kingdom*
[3] *Université Lyon 1, Centre de Recherche Astrophysique de Lyon, 69561 Saint-Genis Laval, France*
[4] *Ecole Normale Supérieure de Lyon, Lyon, France*
[5] *Physics Department, CERN, Geneva CH-1211, Switzerland*
[6] *Tel Aviv University, Department of Physics, P.O. Box 39040, Tel Aviv 6997801, Israel*
[7] *University of Southampton Physics and Astronomy, Southampton SO17 1BJ, United Kingdom*
[8] *SLAC National Accelerator Laboratory, Menlo Park 94025, USA*
[9] *Institute for Particle Physics Phenomenology, Durham University, Durham DH1 3LE, United Kingdom*
[10] *University of Melbourne, Victoria 3010, Australia*
[11] *HH Wills Physics Laboratory, Tyndall Avenue, Bristol BS8 1TH, United Kingdom*
[12] *Rutgers University, Department of Physics and Astronomy, Piscataway, 08854-8019, USA*
[13] *SISSA and INFN, Sezione di Trieste, Trieste 34136, Italy*
[14] *Institute of Theoretical Physics, Chinese Academy of Sciences, Beijing 100190, PR China*
[15] *Service de Physique Théorique, Université Libre de Bruxelles, B-1050, Brussels, Belgium*
[16] *University of California Davis, Department of Physics, 95616, USA*

* Corresponding author.
E-mail address: worm@cern.ch (S. Worm).

http://dx.doi.org/10.1016/j.dark.2015.08.001

[17] Vrije Universiteit Brussel - IIHE, Brussels, Belgium
[18] NIKHEF, Amsterdam, 1098 XG, Netherlands
[19] Universita' di Roma "Sapienza" / INFN, Rome, 00185, Italy
[20] Albert-Ludwigs-Universitaet Physikalisches Institut, Freiburg, 79104, Germany
[21] Université de Genève Ecole de Physique, Geneva, CH-1211, Switzerland
[22] University of Bonn Physikalisches Institut, 53115, Germany
[23] King's College London, Department of Physics, London, WC2R 2LS, United Kingdom
[24] University of Maryland, Department of Physics, College Park, 20742-4111, USA
[25] Rudolf Peierls Centre for Theoretical Physics, University of Oxford, OX1 3NP Oxford, United Kingdom
[26] Physics Division, Argonne National Laboratory, Lemont, 60439, USA
[27] Fermi National Accelerator Laboratory, Batavia, 60510-5011, USA
[28] LPSC, Université Grenoble-Alpes, CNRS/IN2P3, 38042, France
[29] University of California Santa Barbara, Department of Physics, Santa Barbara, 93106, USA
[30] National Centre for Particle Physics, University of Malaya, Kuala Lumpur, 50603, Malaysia
[31] University of Oregon Department of Physics, Eugene, 97403, USA
[32] Harvard University, Department of Physics, Cambridge, 02138, USA
[33] DESY, Notkestrasse 85, D-22607 Hamburg, Germany
[34] Royal Holloway University of London, Department of Physics, Egham, TW20 0EX, United Kingdom
[35] University College London, WC1E 6BT, United Kingdom
[36] The Ohio State University, Columbus, 43210, USA
[37] Texas Tech University, Lubbock, 41051, USA
[38] Physics Department, Brown University, Providence, 02912, USA
[39] GRAPPA, University of Amsterdam, 1098 XH, Netherlands
[40] Enrico Fermi Institute, University of Chicago, 60637, USA
[41] Kavli Institute for Cosmological Physics and the Enrico Fermi Institute, The University of Chicago, 60637, USA
[42] Particle Physics Department, Rutherford Appleton Laboratory, OX11 0QX, United Kingdom
[43] Department of Physics and Astronomy, University of California, Irvine, 92697-4575, USA
[44] KEK, Tsukuba, 305-0801, Japan
[45] University of Glasgow, G12 8QQ, United Kingdom
[46] Berkeley Center for Theoretical Physics, University of California, Berkeley, 94720-7300, USA
[47] Theoretical Physics Group, Lawrence Berkeley National Laboratory, Berkeley, 94720-8162, USA
[48] Bergische Universitaet Wuppertal, D-42119, Germany
[49] University of Zurich Physik-Institut, CH-8057, Switzerland
[50] INFN Sezione di Pavia, 27100, Italy
[51] University of Toronto, Department of Physics, ON M5S 1A7, Canada
[52] University of Oklahoma, Department of Physics, Norman, 73019, USA
[53] Max-Planck-Institut für Kernphysik, Heidelberg, 69117, Germany
[54] Weizmann Institute of Science, Department of Particle Physics and Astrophysics, Rehovot, 7610001, Israel
[55] New York University, Department of Physics, NY, 10003, USA
[56] Perimeter Institute for Theoretical Physics, Waterloo, ON N2L 2Y5, Canada
[57] McMaster University, Department of Physics & Astronomy, Hamilton, ON L8S 4M1, Canada

ARTICLE INFO

Article history:
Received 12 June 2015
Received in revised form
3 August 2015
Accepted 3 August 2015

Keywords:
Dark matter
Direct detection
Collider search for dark matter
Simplified models
Effective field theory

ABSTRACT

This document[a] outlines a set of simplified models for dark matter and its interactions with Standard Model particles. It is intended to summarize the main characteristics that these simplified models have when applied to dark matter searches at the LHC, and to provide a number of useful expressions for reference. The list of models includes both *s*-channel and *t*-channel scenarios. For *s*-channel, spin-0 and spin-1 mediations are discussed, and also realizations where the Higgs particle provides a portal between the dark and visible sectors. The guiding principles underpinning the proposed simplified models are spelled out, and some suggestions for implementation are presented.

1. Introduction

Gravitational effects on astrophysical scales give convincing evidence for the presence of dark matter (DM) in Nature, an observation that is strongly supported by the large-scale structure of the Universe and measurements of the cosmic microwave background [1]. While the existence of DM thus seems well established, very little is known about the properties of the DM particle(s). To shed light on this question, three classes of search strategies are being employed: (i) direct detection in shielded underground detectors; (ii) indirect detection with satellites, balloons, and ground-based telescopes looking for signals of DM annihilation; (iii) particle colliders aiming at direct DM production.

† Primary contributor.
[a] Summary of the discussions and conclusions following from *Dark Matter @ LHC 2014*, held at Merton College, Oxford, on September25–27, 2014.

Despite this intense effort, DM has so far proven elusive. In the coming years, direct and indirect detection will reach new levels of sensitivity, and the LHC will be operating at 13 TeV center-of-mass energy after a very successful 8 TeV run. These upcoming experiments will provide crucial tests of our ideas about DM, and have great potential to revolutionize our understanding of its nature.

Dedicated searches for DM candidates represent an integral part of the physics programme at the LHC. The minimal experimental signature of DM production at a hadron collider consists of an excess of events with a single final-state object X recoiling against large amounts of missing transverse momentum or energy ($\not{E}_T$). In Run I of the LHC, the ATLAS and CMS collaborations have examined a variety of such "mono-X" signatures involving jets of hadrons, gauge bosons, top and bottom quarks as well as the Higgs boson in the final state. A second class of $\not{E}_T$ signatures that has been studied in depth arises from the production of "partner" particles that decay to DM and Standard Model (SM) particles, which usually leads to rather complex final states (for a review of the experimental status after LHC Run I, see for instance [2]).

In order to interpret the cross section limits obtained from the LHC $\not{E}_T$ searches, and to relate these bounds to the constraints that derive from direct and indirect detection, one needs a theory of DM. In fact, as illustrated in Fig. 1, one can construct not just one, but a large number of qualitatively different DM models. Collectively these models populate the "theory space" of all possible realizations of physics beyond the SM with a particle that is a viable DM candidate. The members of this theory space fall into three distinct classes:

(I) On the simple end of the spectrum, we have theories where the DM may be the only accessible state to our experiments. In such a case, effective field theory (EFT) allows us to describe the DM–SM interactions mediated by all kinematically inaccessible particles in a universal way. The DM–EFT approach [3–10] has proven to be very useful in the analysis of LHC Run I data, because it allows to derive stringent bounds on the "new-physics" scale Λ that suppresses the higher-dimensional operators. Since for each operator a single parameter encodes the information on all the heavy states of the dark sector, comparing LHC bounds to the limits following from direct and indirect DM searches is straightforward in the context of DM–EFTs.

(II) The large energies accessible at the LHC call into question the momentum expansion underlying the EFT approximation [6,10–17], and we can expand our level of detail toward simplified DM models (for early proposals see for example [18–23]). Such models are characterized by the most important state mediating the DM particle interactions with the SM, as well as the DM particle itself. Unlike the DM–EFTs, simplified models are able to describe correctly the full kinematics of DM production at the LHC, because they resolve the EFT contact interactions into single-particle s-channel or t-channel exchanges. This comes with the price that they typically involve not just one, but a handful of parameters that characterize the dark sector and its coupling to the visible sector.

(III) While simplified models capture some set of signals accurately at LHC energies (and beyond), they are likely to miss important correlations between observables. Complete DM models close this gap by adding more particles to the SM, most of which are not suitable DM candidates. The classical example is the Minimal Supersymmetric SM (MSSM), in which each SM particle gets its own superpartner and the DM candidate, the neutralino, is a weakly interacting massive particle. Reasonable phenomenological models in this class have of order 20 parameters, leading to varied visions of DM. At the same time, they build-in correlations from symmetry-enforcing relations among couplings, that would look like random accidents in a simplified model description. Complete DM models can in principle answer any question satisfactorily, but one might worry that their structure is so rich that it is impossible to determine unambiguously the underlying new dynamics from a finite amount of data ("inverse problem") [24].

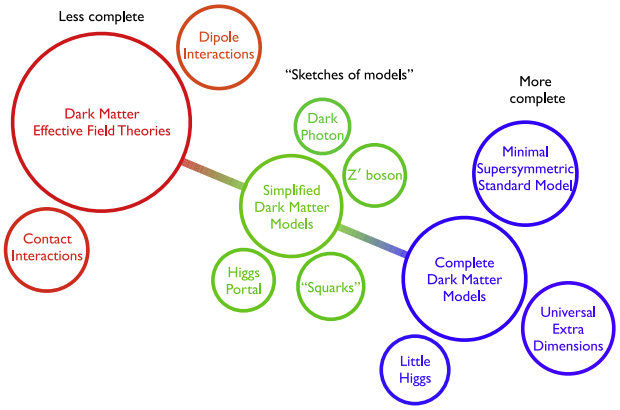

Fig. 1. Artistic view of the DM theory space. See text for detailed explanations.

Given our ignorance of the portal(s) between the dark sector and the SM, it is important that we explore *all* possibilities that the DM theory space has to offer. While the three frameworks discussed above have their own *pros* and *cons*, they are all well-motivated, interesting, and each could, on its own, very well lead to breakthroughs in our understanding of DM. Ignoring whole "continents" of the DM theory landscape at Run II, say EFTs, would be shortsighted, and might well make it impossible to exploit the full LHC potential as a DM discovery machine.

In recent years, a lot of progress has been made in exploring and understanding both DM–EFTs and a variety of complete models. The same cannot (yet) be said about simplified models that bridge between the two ends of the spectrum in theory space. Following the spirit of [25,26], we attempt in this document to lay the theoretical groundwork that should be useful for the DM@LHC practitioner. We begin in Section 2 by discussing the general criteria that a simplified DM model should fulfill to make it useful at the LHC. This section contains in addition an explanation of the concept of Minimal Flavor Violation (MFV) [27–30] and its importance to model building as well as a brief note on the relevance of the spin of the DM particle for LHC searches. Simplified spin-0 s-channel models are then described in Section 3. Since these scenarios can be understood as limiting cases of Higgs portal models, we provide in Section 4 a summary of the most important representatives of these theories. Section 5 is devoted to simplified spin-1 s-channel models, while Section 6 deals with t-channel scenarios. To make the work self-contained, we not only discuss the LHC phenomenology of each simplified model, but also provide the relevant formulas to analyze the constraints from direct detection and annihilation of DM. We conclude and provide an outlook in Section 7.

2. Criteria for simplified models

For a simplified DM model to be useful at the LHC, it should fulfill the following three criteria: (i) it should be simple enough to form a credible unit within a more complicated model; (ii) it should be complete enough to be able to describe accurately the relevant physics phenomena at the energies that can be probed at the LHC; (iii) by construction it should satisfy all non high-p_T constraints in most of its parameter space.

One way to guarantee that these three criteria are met consists in putting the following requirements/restrictions on the particle content and the interactions of the simplified model:

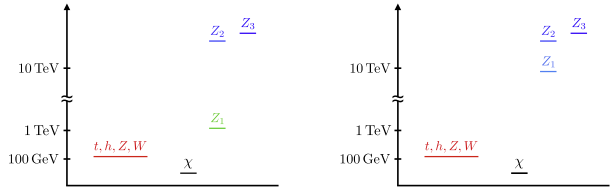

Fig. 2. Left: Schematic mass spectrum of a simplified DM model. In the case considered, the DM particle χ is lighter than the heaviest SM particles t, h, Z, W. The lightest mediator state is called Z_1 and can be produced on-shell at the LHC. The remaining dark-sector states Z_2 and Z_3 are separated by a mass gap from Z_1 and inaccessible. Right: The EFT limit of the simplified model with a decoupled mediator Z_1. See text for further details.

(I) Besides the SM, the model should contain a DM candidate that is either absolutely stable or lives long enough to escape the LHC detectors, as well as a mediator that couples the two sectors. The dark sector can be richer, but the additional states should be somewhat decoupled. A typical mass spectrum is sketched on the left in Fig. 2.

(II) The Lagrangian should contain (in principle) all terms that are renormalizable and consistent with Lorentz invariance, the SM gauge symmetries, and DM stability. However, it may be permissible to neglect interactions or to study cases where couplings are set equal to one another. If such simplifications are made, one should however try to verify that these approximations do not result in a very different DM phenomenology and they should be spelled out clearly in the text and on all relevant plots.

(III) The additional interactions should not violate the exact and approximate accidental global symmetries of the SM. This means that the interactions between the visible and the dark sector should be such that baryon and lepton number is conserved and that the custodial and flavor symmetries of the SM are not strongly broken.

Simplified models are thus specifically designed to involve only a few new particles and interactions, and many of them can be understood as a limit of a more general new-physics scenario, where all but the lightest dark-sector states are integrated out. By construction, the physics of simplified models can therefore be characterized in terms of a small number of parameters such as particle masses and couplings. While simplified models are clearly not model-independent, they do avoid some pitfalls of DM–EFTs. In particular, they allow one to correctly describe the kinematics of DM production at the LHC, by virtue of the dynamical mediator(s) that they contain. Conversely, by making the mediator(s) sufficiently heavy the EFT framework can be recovered. The latter feature is illustrated on the left-hand side of Fig. 2.

2.1. Note about flavor and CP violation

The requirement (III) deserves further explanations. The SM possesses both exact and approximate global accidental symmetries. The former (baryon and lepton number) are conserved at the renormalizable level, while the latter (custodial and flavor symmetries) are broken by quantum effects, but parametrically small in the sense that they become exact global symmetries when a parameter or a number of parameters are set to zero. New physics will generically not respect these accidental symmetries and, as a result, its parameter space will be severely constrained: the new interactions are required to be weak or the new states have to be heavy (or both).

A systematic way to curb the size of dangerous flavor-violating and CP-violating effects consists in imposing MFV. Loosely speaking the idea behind MFV is that the general structure of flavor-changing neutral current (FCNC) processes present in the SM is preserved by new physics. In particular, all flavor-violating and CP-violating transitions are governed by the Cabibbo–Kobayashi–Maskawa (CKM) matrix. This basic idea can be formalized and formulated in an EFT [30]. Employing the EFT language, a new-physics model satisfies the MFV criterion if the additional interactions in the quark sector are either invariant under the global SM flavor group $G_q = U(3)_q \times U(3)_u \times U(3)_d$, or any breaking is associated with the quark Yukawa matrices Y^u and Y^d. The notion of MFV can be also be extended to the case of CP violation and to the lepton sector — although for leptons its definition is not unique, if one wants to accommodate neutrino masses.

2.1.1. MFV spin-0 s-channel models

To understand which restrictions MFV imposes on the flavor structure of simplified models, we work out some examples relevant for the discussions in later sections. We begin with a very simple model in which DM is a real scalar (gauge and flavor) singlet χ and the SM Higgs doublet H provides a portal to the dark sector of the form $\chi^2|H|^2$ (the most important phenomenological implications of this scenario will be discussed in Section 4.2). Following the notion of MFV, the interaction terms between the mediator and the quark fields should be either invariant under G_q or break it only via Y^u or Y^d. Given the transformation properties $q \sim (3,1,1)$, $u \sim (1,3,1)$ and $d \sim (1,1,3)$, it follows that the combination $\bar{q}u$ of left-handed and right-handed quark fields breaks $U(3)_q \times U(3)_u$, while the bilinear $\bar{q}d$ breaks $U(3)_q \times U(3)_d$. This means that we have to go with the second option. In terms of gauge eigenstates, we write

$$\mathcal{L} \supset -\sum_{i,j}\Big((Y^u)_{ij}\bar{q}_i H u_j + (Y^d)_{ij}\bar{q}_i \tilde{H} d_j + \text{h.c.}\Big), \tag{1}$$

where i,j runs over the three quark families, $\tilde{H}_a = \epsilon_{ab}H^b$ with $a,b = 1,2$ and the two terms involve the Higgs fields to make them $SU(2)_L \times U(1)_Y$ gauge invariant. Notice that the above interactions are invariant under G_q, if the Yukawa matrices are promoted to non-dynamical fields (spurions) with the following transformation properties $Y^u \sim (3,\bar{3},1)$ and $Y^d \sim (3,1,\bar{3})$.

Having constructed the couplings between the mediator and the quarks in the gauge basis, one still has to transform to the mass eigenstate basis. In the case of (1) the final result of this transformation is obvious, because the Lagrangian is simply the quark part of the Yukawa sector of the SM. One finds

$$\mathcal{L} \supset -\frac{h}{\sqrt{2}}\sum_i\Big(y_i^u \bar{u}_i u_i + y_i^d \bar{d}_i d_i\Big), \tag{2}$$

where h is the physical Higgs field and $y_i^q = \sqrt{2}m_i^q/v$ with $v \simeq 246$ GeV the vacuum expectation value (VEV) of H that breaks the electroweak symmetry. The lesson to learn from this exercise is that in order to construct MFV simplified models that describe s-channel exchange of spin-0 resonances, the portal couplings to the SM fermions should be of Yukawa type. The above line of reasoning will be applied to the simplified models in Section 3.

2.1.2. MFV spin-1 s-channel models

The second example that we want to discuss is even simpler than the first one. We consider the interactions of DM in form of a Dirac fermion χ with the SM quarks through the exchange of spin-1 mediators which we call Z'. MFV does not restrict the couplings between the mediator and DM, and as a consequence the interactions take the generic form $Z'_\mu\left(g_L^\chi\,\bar{\chi}\gamma^\mu P_L\chi + g_R^\chi\,\bar{\chi}\gamma^\mu P_R\chi\right)$ with $P_{L,R} = (1 \mp \gamma_5)/2$ denoting left-handed and right-handed chiral projectors. Since the bilinears $\bar{q}\gamma^\mu q$, $\bar{u}\gamma^\mu u$, and $\bar{d}\gamma^\mu d$ are all

flavor singlets, we do not have to invoke the Yukawa couplings Y^u and Y^d, and simply write

$$\mathcal{L} \supset Z'_\mu \sum_i \Big[g_L^q \left(\bar{u}_i \gamma^\mu P_L u_i + \bar{d}_i \gamma^\mu P_L d_i\right) + g_R^u \bar{u}_i \gamma^\mu P_R u_i + g_R^d \bar{d}_i \gamma^\mu P_R d_i \Big]. \tag{3}$$

In fact, this expression holds both in the gauge as well as the mass eigenstate basis as long as the coefficients g_L^q, g_R^u, and g_R^d are flavor independent. Notice that (3) contains the case of pure vector or axialvector quark couplings as a special case, i.e. $g_L^q = g_R^u = g_R^d$ or $g_L^q = -g_R^u = -g_R^d$, respectively. Spin-1 *s*-channel simplified models of MFV type will be discussed in Section 5.

2.1.3. Comment on non-MFV models

For the sake of argument let us also consider an example of a simplified model that does not conform with MFV. As a toy-model we take a Z' boson that couples vectorial to the quark gauge eigenstates, but differently to the first, compared to the second and third generations. We parameterize this non-universality by a real parameter Δ_V, and restrict ourselves to down-type quarks writing

$$\mathcal{L} \supset Z'_\mu \sum_i \left(g_V + \Delta_V \delta_{i1}\right) \bar{d}_i \gamma^\mu d_i. \tag{4}$$

To go to the mass eigenstate basis requires rotating the left-handed and right-handed quark fields by 3×3 unitarity matrices $U_{L,R}^{u,d}$. These rotations will leave the term proportional to g_V flavor diagonal, but will induce flavor off-diagonal terms of the form

$$\mathcal{L} \supset Z'_\mu \, \Delta_V \sum_{i,j} \left(L_{ij} \bar{d}_i \gamma^\mu P_L d_j + R_{ij} \bar{d}_i \gamma^\mu P_R d_j\right) \tag{5}$$

with

$$L = U_L^{d\,\dagger} \,\mathrm{diag}\,(1,0,0)\, U_L^d, \qquad R = U_R^{d\,\dagger} \,\mathrm{diag}\,(1,0,0)\, U_R^d. \tag{6}$$

At this point we have to make some assumptions about the flavor structure of the ultraviolet (UV) complete model that gives rise to (4) to progress further. Since the right-handed rotations $U_R^{u,d}$ are not observable in the SM, we assume that U_R^d is the 3×3 unit matrix 1_3. This implies that $R = \mathrm{diag}\,(1,0,0)$ and thus there are no FCNCs in the right-handed down-quark sector. In contrast, the left-handed rotations are observable in the SM, because they combine to give the CKM matrix, i.e. $V = U_L^{u\,\dagger} U_L^d$. A possible simple choice that satisfies this requirement is $U_L^d = V$ and $U_L^u = 1_3$, resulting in

$$L = \begin{pmatrix} |V_{ud}|^2 & V_{ud}^* V_{us} & V_{ud}^* V_{ub} \\ V_{us}^* V_{ud} & |V_{us}|^2 & V_{us}^* V_{ub} \\ V_{ub}^* V_{ud} & V_{ub}^* V_{us} & |V_{ub}|^2 \end{pmatrix}, \tag{7}$$

which implies flavor violation in the down-type quark sector. Note that choosing $U_L^d = 1_3$ and $U_L^u = V^\dagger$ would give $L = \mathrm{diag}\,(1,0,0)$. However, this choice does not solve the new-physics "flavor problem", because it is easy to see that FCNCs would then appear in the up-type quark sector.

Using (7) it is straightforward to calculate the FCNCs induced by tree-level Z'-boson exchange. For instance, the new-physics amplitude relevant for kaon mixing can be estimated to be

$$\mathcal{A}(s\bar{d} \to Z' \to \bar{s}d) \sim \frac{(V_{ud}^* V_{us})^2 \Delta_V^2}{M_{Z'}^2} \simeq 5 \times 10^{-2} \, \frac{\Delta_V^2}{M_{Z'}^2} \tag{8}$$

with M_Z' the mass of the Z' boson. This result should be compared to the dominant SM contribution to K–$\bar{K}$ mixing, which arises from top-W boxes and is given by

$$\mathcal{A}(s\bar{d} \to \mathrm{box} \to \bar{s}d) \sim \frac{\alpha_w^2 \left(V_{td}^* V_{ts}\right)^2 y_t^2}{256 M_W^2} \simeq \frac{5 \times 10^{-13}}{M_W^2}, \tag{9}$$

with $\alpha_w = g^2/(4\pi)$ the weak coupling constant, M_W the W-boson mass, and $y_t \simeq 1$ the top Yukawa. A rough bound on the amount of additional flavor violation $\Delta_V/M_{Z'}$ can now be obtained by simply requiring that (8) should be smaller in magnitude than (9). It follows that

$$\left| \frac{\Delta_V M_W}{M_{Z'}} \right| \lesssim 3 \times 10^{-6}, \tag{10}$$

which implies that for $\Delta_V \simeq 1$ the Z'-boson mass $M_{Z'}$ should be larger than around 3×10^4 TeV, because otherwise one would be in conflict with the experimental bounds on kaon mixing. In view of this result it should be clear that in order to allow for interesting LHC phenomenology, one has to require that the simplified model is MFV. In our toy model (4) this is simply achieved by setting $\Delta_V = 0$. We finally add that for very light mediators important constraints on simplified models can however still arise from quark-flavor physics even if their interactions are MFV (see [31] for a recent comprehensive discussion).

2.2. Note about spins

In many cases, there will be variations of the simplified model under consideration where the DM is a real or complex scalar, Dirac or Majorana fermion, or even a neutral vector. In some cases, even simple changes such as considering a Majorana instead of a Dirac fermion can lead to big changes in the phenomenology of direct detection experiments and/or annihilation. The classical examples are that for Majorana fermions the vector coupling vanishes identically and that such DM particles cannot have an electric or magnetic dipole moment. In the context of simple cut-and-count analyses at the LHC, the precise nature of the DM particle is generically less relevant in the sense that it will to first order only affect the total production cross sections. Angular observables that are sensitive to the structure of the dark sector have however been constructed and studied [32–34], but such analyses necessarily involve topologies beyond $2 \to \not{E}_T + 1$.

3. Scalar *s*-channel mediator

A scalar particle mediator can be a very simple addition to the SM. If it is chosen as a gauge singlet, it can have tree-level interactions with a singlet DM particle that is either a Dirac or Majorana fermion, or DM that is itself a scalar. The spin-0 mediator could still be chosen as either a real or complex scalar, which are distinguished by the fact that a complex scalar contains both scalar and pseudoscalar particles, whereas the real option contains only the scalar field. We will consider here two choices for DM simplified models: one where the interaction with the SM is mediated by the real scalar, and the second where we consider only a light pseudoscalar (assuming that the associated scalar is decoupled from the low-energy spectrum).

Couplings to the SM fermions can be arranged by mixing with the SM Higgs. Such models have intriguing connections with Higgs physics, and can be viewed as generalizations of the Higgs portal to DM. The impact on Higgs physics is discussed in Section 4.2. The most general scalar mediator models will of course have renormalizable interactions between the SM Higgs and the new scalar ϕ or pseudoscalar a, as well as ϕ/a interactions with electroweak gauge bosons. Such interactions are model-dependent, often subject to constraints from electroweak precision tests, and would suggest specialized searches which cannot be generalized to a broad class of models (unlike, for instance, the $\not{E}_T + j$ searches). As a result, for this class of simplified models with spin-0 mediators, we suggest to focus primarily on the couplings to fermions and the loop-induced couplings to gluons. The possibility that the couplings to the electroweak sector can also lead to interesting DM phenomenology should however be kept in mind, and can be studied in the context of Higgs portal DM.

3.1. Fermionic DM

MFV dictates that the coupling of a scalar to the SM fermions will be proportional to the fermion masses. However, it allows these couplings to be scaled by separate factors for the up-type quarks, down-type quarks, and the charged leptons. Assuming that DM is a Dirac fermion χ, which couples to the SM only through a scalar ϕ or pseudoscalar a, the most general tree-level Lagrangians compatible with the MFV assumption are [23,35]:

$$\mathcal{L}_{\text{fermion},\phi} \supset -g_\chi \phi \bar{\chi}\chi - \frac{\phi}{\sqrt{2}} \sum_i \left(g_u y_i^u \bar{u}_i u_i + g_d y_i^d \bar{d}_i d_i + g_\ell y_i^\ell \bar{\ell}_i \ell_i \right), \tag{11}$$

$$\mathcal{L}_{\text{fermion},a} \supset -i g_\chi a \bar{\chi}\gamma_5\chi - \frac{ia}{\sqrt{2}} \sum_i \left(g_u y_i^u \bar{u}_i \gamma_5 u_i + g_d y_i^d \bar{d}_i \gamma_5 d_i + g_\ell y_i^\ell \bar{\ell}_i \gamma_5 \ell_i \right). \tag{12}$$

Here the sums run over the three SM families and we are using Yukawa couplings y_i^f normalized as $y_i^f = \sqrt{2} m_i^f / v$ with v the Higgs VEV. We parameterize the DM-mediator coupling by g_χ, rather than by a Yukawa coupling $y_\chi = \sqrt{2} m_\chi / v$, since the DM particle χ most likely receives its mass from other (unknown) mechanisms, rather than electroweak symmetry breaking.

The most general Lagrangians including new scalars or pseudoscalars will have a potential containing interactions with the SM Higgs field h. As stated above, we choose to take a more minimal set of possible interactions, and leave the discussions of the couplings in the Higgs sector to the section on Higgs portal DM. Given this simplification, the minimal set of parameters under consideration is

$$\left\{ m_\chi,\ m_{\phi/a},\ g_\chi,\ g_u,\ g_d,\ g_\ell \right\}. \tag{13}$$

The simplest choice of couplings is $g_u = g_d = g_\ell$, which is realized in singlet scalar extensions of the SM (see Section 4.2). If one extends the SM Higgs sector to a two-Higgs-doublet model, one can obtain other coupling patterns such as $g_u \propto \cot\beta$ and $g_d \propto g_e \propto \tan\beta$ with $\tan\beta$ denoting the ratio of VEVs of the two Higgs doublets. The case $g_u \neq g_d \neq g_\ell$ requires additional scalars, whose masses could be rather heavy. For simplicity, we will use universal couplings $g_v = g_u = g_d = g_\ell$ in the remainder of this section, though one should bear in mind that finding ways to test this assumption experimentally would be very useful.

The signal strength in DM pair production does not only depend on the masses m_χ and $m_{\phi/a}$ and the couplings g_i, but also on the total decay width of the mediator ϕ/a. In the minimal model as specified by (11) and (12), the widths for the mediators are given by:

$$\Gamma_\phi = \sum_f N_c \frac{y_f^2 g_v^2 m_\phi}{16\pi} \left(1 - \frac{4m_f^2}{m_\phi^2}\right)^{3/2} + \frac{g_\chi^2 m_\phi}{8\pi} \left(1 - \frac{4m_\chi^2}{m_\phi^2}\right)^{3/2} + \frac{\alpha_s^2 g_v^2 m_\phi^3}{32\pi^3 v^2} \left| f_\phi\left(\frac{4m_t^2}{m_\phi^2}\right)\right|^2, \tag{14}$$

$$\Gamma_a = \sum_f N_c \frac{y_f^2 g_v^2 m_a}{16\pi} \left(1 - \frac{4m_f^2}{m_a^2}\right)^{1/2} + \frac{g_\chi^2 m_a}{8\pi} \left(1 - \frac{4m_\chi^2}{m_a^2}\right)^{1/2} + \frac{\alpha_s^2 g_v^2 m_a^3}{32\pi^3 v^2} \left| f_a\left(\frac{4m_t^2}{m_\phi^2}\right)\right|^2, \tag{15}$$

with

$$f_\phi(\tau) = \tau \left[1 + (1-\tau)\arctan^2\left(\frac{1}{\sqrt{\tau - 1}}\right)\right], \qquad f_a(\tau) = \tau \arctan^2\left(\frac{1}{\sqrt{\tau - 1}}\right). \tag{16}$$

The first term in each width corresponds to the decay into SM fermions (the sum runs over all kinematically accessible fermions, $N_c = 3$ for quarks and $N_c = 1$ for leptons). The second term is the decay into DM (assuming that this decay is kinematically allowed). The factor of two between the decay into SM fermions and into DM is a result of our choice of normalization of the Yukawa couplings. The last term corresponds to decay into gluons. Since we have assumed that $g_v = g_u = g_d = g_\ell$, we have included in the partial decay widths $\Gamma(\phi/a \to gg)$ only the contributions stemming from top loops, which provide the by far largest corrections given that $y_t \gg y_b$, etc. At the loop level the mediators can decay not only to gluons but also to pairs of photons and other final states if these are kinematically accessible. The decay rates $\Gamma(\phi/a \to gg)$ are however always larger than the other loop-induced partial widths, and in consequence the total decay widths $\Gamma_{\phi/a}$ are well approximated by the corresponding sum of the individual partial decay widths involving DM, fermion or gluon pairs. Notice finally that if $m_{\phi/a} > 2m_t$ and $g_u \gtrsim g_\chi$ the total widths of ϕ/a will typically be dominated by the partial widths to top quarks.

3.1.1. LHC searches

Under the assumption of MFV, supplemented by $g_v = g_u = g_d = g_\ell$, the most relevant couplings between DM and the SM arising from (11) and (12) are those that involve top quarks. Two main strategies have been exploited to search for scalar and pseudoscalar interactions of this type using LHC data. The first possibility consists in looking for a mono-jet plus missing energy signal $\not{E}_T + j$, where the mediators that pair produce DM are radiated from top-quark loops [36], while the second possibility relies on detecting the top-quark decay products that arise from the tree-level reaction $\not{E}_T + t\bar{t}$ [37]. In the first paper [36] that discussed the $\not{E}_T + j$ signal the effects of DM fermions coupled to heavy-quark loops were characterized in terms of effective higher-dimensional operators, i.e. with mediators being integrated out. The effects of dynamical scalar and pseudoscalar messengers in the s-channel mediating interactions between the heavy quarks in the loop and DM were computed in characterizing the LHC signatures for DM searches in [38,33,39–41].

Final states involving top-quark pairs were considered in the articles [42–45,39,41]. Searches for a $\not{E}_T + b\bar{b}$ signal [37,42,45] also provide an interesting avenue to probe (11) and (12), while the constraints from mono-jet searches on the scalar and pseudoscalar interactions involving the light quark flavors are very weak due to the strong Yukawa suppression (as discussed in detail in [38,46]), and thus are unlikely to be testable at the LHC. Scenarios where the DM–SM interactions proceed primarily via gluons have also been considered [47].

Predicting mono-jet cross sections in the simplified models (11) and (12) is complicated by the fact that the highly energetic initial-state and/or final-state particles involved in the process are able to resolve the structure of the top-quark loops that generate the $\not{E}_T + j$ signal (see the left-hand side of Fig. 3). Integrating out the top quark and describing the interactions by an effective operator of the form $\phi G^a_{\mu\nu} G^{a,\mu\nu}$ ($a G^a_{\mu\nu} \tilde{G}^{a,\mu\nu}$) with $G^a_{\mu\nu}$ the field strength tensor of QCD and $\tilde{G}^{a,\mu\nu} = 1/2 \epsilon^{\mu\nu\lambda\rho} G^a_{\lambda\rho}$ its dual, is in such a situation a poor approximation [36,38]. Already in the LHC Run I environment the $m_t \to \infty$ limit overestimates the exact cross sections by a factor of 5 (40) for $m_\chi \simeq 10$ GeV ($m_\chi \simeq 1$ TeV) [41]. Removing the top quark as an active degree of freedom becomes even less justified at 13 (14) TeV, where the $\not{E}_T$ and $p_{T,j}$ selection requirements have to be harsher than at (7) 8 TeV to differentiate the DM signal from the SM background. In order to infer reliable bounds on (11) and (12), one therefore has to calculate the mono-jet cross section keeping the full top-quark mass dependence. Such calculations are now publicly available at leading order (LO) in MCFM [38] and at LO plus

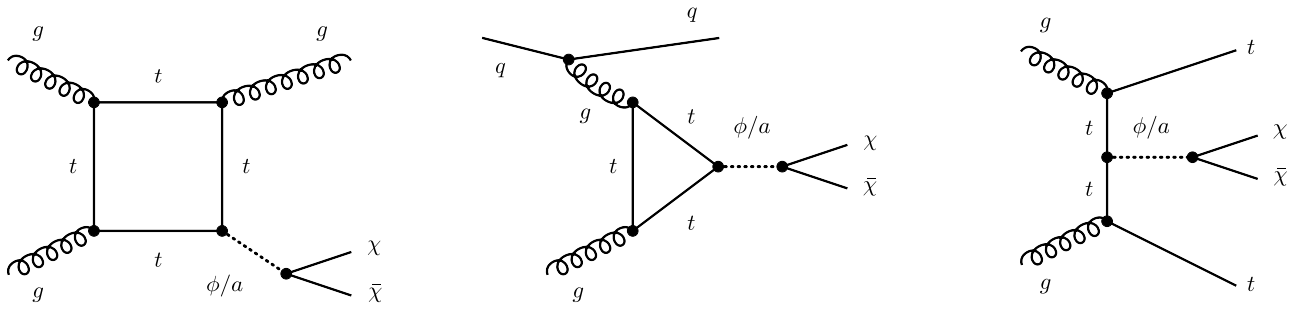

Fig. 3. Left: Two examples of one-loop diagrams with an exchange of a ϕ/a mediator that provide the dominant contribution to a mono-jet signature. Right: A tree-level graph that leads to a $\not{E}_T + t\bar{t}$ signal.

parton shower (LOPS) in the POWHEG BOX [41]. Given that the $\not{E}_T + t\bar{t}$ ($b\bar{b}$) signals arise in the context of (11) and (12) at tree level (see the right-hand side of Fig. 3), event generation through programs like MadGraph5 [48] is possible, and UFO model files [49] from different groups [39–41] are available for this purpose.

Since (11) and (12) is a simplified DM model, it is possible that the mediator can decay into additional states present in the full theory that we have neglected. For example, ϕ/a may decay into new charged particles which themselves eventually decay into DM, but with additional visible particles that would move the event out of the selection criteria of the mono-jet or similar $\not{E}_T$ searches. Another possibility is that the mediator can also decay invisibly into other particles of the dark sector. In either case, the expressions for $\Gamma_{\phi/a}$ as given in (14) and (15) are lower bounds on the total decay-width of the mediators. To understand how the actual value of $\Gamma_{\phi/a}$ influences the LHC sensitivity, one has to recall that for $m_{\phi/a} \ll \sqrt{\hat{s}}$ (where $\sqrt{\hat{s}}$ is some characteristic fraction of the center-of-mass energy of the collider in question) and $m_{\phi/a} > 2m_\chi$, DM-pair production proceeds dominantly via an on-shell mediator. If the narrow width approximation (NWA) is applicable, the mono-jet cross section factorizes into a product of on-shell production of ϕ/a times its branching ratio into $\chi\bar{\chi}$, i.e. $\sigma(pp \to \not{E}_T + j) = \sigma(pp \to \phi/a + j)\,\mathrm{Br}(\phi/a \to \chi\bar{\chi})$. One can draw three conclusions from this result. First, in the parameter region where $m_{\phi/a} > 2m_\chi$ and $\Gamma_{\phi/a} \ll m_{\phi/a}$, a change in $\Gamma_{\phi/a}$ will simply lead to a rescaling of the cross section, namely $\sigma(pp \to \not{E}_T + j) \propto 1/\Gamma_{\phi/a}$. This implies in particular that kinematic distributions of simple $\not{E}_T$ signals will to first approximation be unaltered under variations of $\Gamma_{\phi/a}$. Second, for parameter choices where the partial decay width to $\bar{\chi}\chi$ DM pairs is dominant, the cross section scales as $\sigma(pp \to \not{E}_T + j) \propto g_v^2$. If the partial decay width to SM particles gives the largest contribution to $\Gamma_{\phi/a}$, one has instead $\sigma(pp \to \not{E}_T + j) \propto g_\chi^2$. Third, the scaling $\sigma(pp \to \not{E}_T + j) \propto g_\chi^2 g_v^2$ only holds for off-shell production, which occurs for $m_{\phi/a} < 2m_\chi$. Notice that for $m_{\phi/a} \lesssim 2m_\chi$, the total decay width of ϕ/a will have a non-trivial impact on the constraints that the LHC can set, since the amount of off-shell production depends sensitively on $\Gamma_{\phi/a}$.

Similarly, the total decay width effect is non-trivial when the mediator can decay into other particles in the invisible sector beyond the cosmologically stable DM. To apply the simplified models framework to these scenarios, it was proposed in [39,40] to treat the mediator width as an independent parameter in the simplified model characterization.

We now turn to the constraints on these models from non-collider experiments: thermal relic abundance, indirect detection, and direct detection. The first two results can be considered together, as they depend on the same set of annihilation cross sections.

3.1.2. Thermal cross sections

The thermally-average annihilation of DM through the spin-0 mediators can be calculated from the simplified model (11) and (12). The resulting cross sections for annihilation into SM fermions are given by

$$(\sigma v)(\chi\bar{\chi} \to \phi \to f\bar{f}) = N_c \frac{3 g_\chi^2 g_v^2 y_f^2 m_\chi T}{8\pi\left[(m_\phi^2 - 4m_\chi^2)^2 + m_\phi^2 \Gamma_\phi^2\right]} \times \left(1 - \frac{m_f^2}{m_\chi^2}\right)^{3/2}, \tag{17}$$

$$(\sigma v)(\chi\bar{\chi} \to a \to f\bar{f}) = N_c \frac{g_\chi^2 g_v^2 y_f^2 m_\chi^2}{4\pi\left[(m_a^2 - 4m_\chi^2)^2 + m_a^2 \Gamma_a^2\right]} \times \left(1 - \frac{m_f^2}{m_\chi^2}\right)^{1/2}, \tag{18}$$

where T denotes the DM temperature. Notably, scalar mediators do not have a temperature-independent contribution to their annihilation cross section, while pseudoscalars do. As $T \propto v^2$ (where v is the DM velocity), there is no velocity-independent annihilation through scalars. In the Universe today $v \simeq 1.3 \times 10^{-3} c$, so there are no non-trivial constraints on DM annihilation from indirect detection in the scalar mediator model (see, however, Refs. [50,51]).

The parameter space of the pseudoscalar model, on the other hand, can be constrained by indirect detection. Most constraints from indirect detection are written in terms of a single annihilation channel, and so the constraints for the full simplified model (with multiple annihilation channels open) require some minor modifications of the available results. In the case at hand, good estimates can be obtained by considering the most massive fermion into which the DM can annihilate (bottom and top quarks if they are accessible), as they dominate the annihilation cross section. Note that, away from resonance, the total width Γ_a entering in (18) is relatively unimportant for obtaining the correct indirect detection constraints.

The thermal relic calculation requires the same input cross sections as indirect detection. Here, the cross sections are summed over all kinematically available final states, and can be written as

$$\langle \sigma v \rangle = a + bT. \tag{19}$$

If the DM particles are Dirac fermions, one has to include a factor of 1/2 in the averaging, because Dirac fermions are not their own anti-particles. In the Majorana case no such factor needs to be taken into account. The thermal relic abundance of DM is then

$$\Omega_\chi h^2 = 0.11 \frac{7.88 \times 10^{-11} x_f \ \mathrm{GeV}^{-2}}{a + 3b/x_f}, \tag{20}$$

where $x_f = m_\chi/T_f \in [20, 30]$ with T_f the freeze-out temperature. For reasonable early Universe parameters, the correct relic abundance $\Omega_\chi h^2 \simeq 0.11$ occurs in the ballpark of

$$3 \times 10^{-26}\,\mathrm{cm}^3/\mathrm{s} = 2.57 \times 10^{-9}\,\mathrm{GeV}^{-2} = a + 3b/x_f. \tag{21}$$

Keep in mind that these equations require some modification when the DM-mediator system is on resonance. Further, recall that it is unknown whether or not DM is a thermal relic, or if the only annihilation process in play in the early Universe proceeds through the mediator considered in the simplified model. Therefore, while it is appropriate to compare the sensitivity of experimental results to the thermal cross section, this is not the only range of parameters of theoretical interest.

3.1.3. Direct detection

In contrast to the situation discussed before, elastic scattering of DM on nucleons induced by ϕ/a exchange can be very well described in terms of an EFT. Integrating out the mediators leads to the expressions

$$O_\phi = \frac{g_\chi g_v y_q}{\sqrt{2} m_\phi^2}\,\bar\chi\chi\bar q q, \qquad O_a = \frac{g_\chi g_v y_q}{\sqrt{2} m_a^2}\,\bar\chi\gamma_5\chi\bar q\gamma_5 q, \tag{22}$$

at tree level, as well as contact terms consisting of four DM or quark fields. Removing the top quark as an active degree of freedom generates an effective interaction between DM and gluons. At the one-loop level, one obtains

$$O_G = \frac{\alpha_s\, g_\chi g_v}{12\pi\, v m_\phi^2}\,\bar\chi\chi G^a_{\mu\nu}G^{a,\mu\nu}, \quad O_{\tilde G} = \frac{\alpha_s g_\chi g_v}{8\pi\, v m_a^2}\,\bar\chi\gamma_5\chi G^a_{\mu\nu}\tilde G^{a,\mu\nu}, \tag{23}$$

by employing the Shifman–Vainshtein–Zakharov relations [52]. At the bottom- and charm-quark threshold, one has to integrate out the corresponding heavy quark by again applying (23). Note that this matching procedure is crucial to obtain the correct DM-nucleon scattering cross section associated with effective spin-0 DM-quark interactions.

The DM scattering cross section with nuclei is then obtained by calculating the nucleon matrix elements of the operators (22) and (23) at a hadronic scale of the order of 1 GeV. Direct detection provides relevant constraints only on the scalar mediator model and not the pseudoscalar case, since only the operators O_ϕ and O_G lead to a spin-independent (SI) cross section, while for O_a and $O_{\tilde G}$ the DM-nucleon scattering turns out to be spin-dependent (SD) and momentum-suppressed.

The scalar interactions with the nuclear targets used for direct detection are (to good approximation) isospin-conserving, so that the elastic DM-nucleon cross section can be written as ($N = n, p$)

$$\sigma^{\mathrm{SI}}_{\chi-N} = \frac{\mu^2_{\chi-N} m_N^2}{\pi}\left(\frac{g_\chi g_v}{v m_\phi^2}\right)^2 f_N^2, \tag{24}$$

where $\mu_{\chi-N}$ is the DM-nucleon reduced mass $\mu_{\chi-N} = m_\chi m_N/(m_\chi + m_N)$ and $m_N \simeq 0.939$ GeV is the average nucleon mass. The form factor f_N is given by

$$f_N = \sum_{q=u,d,s} f_N^q + \frac{2}{9} f_N^G \simeq 0.3, \tag{25}$$

where the numerical value has been obtained using $f_N^u \simeq 0.017$, $f_N^d \simeq 0.036$, $f_N^s \simeq 0.043$ [53,54] and $f_N^G = 1 - \sum_{q=u,d,s} f_N^q \simeq 0.904$. Notice that the constraints arising from existing and future direct limits on (24) can be evaded by assuming that χ is not stable on cosmological time scales, but lives long enough to escape the ATLAS and CMS detectors. When comparing the bounds set by direct detection and the LHC, this loophole should be kept in mind.

4. Higgs portal DM

DM may predominantly couple to the SM particles through the SM Higgs. There are three broad classes of models of this kind:

A. The DM particle is a scalar singlet under the SM gauge group, which couples through a quartic interaction with the Higgs. The collider phenomenology of this DM scenario has been extensively studied in the literature (see for instance [55–61]).
B. The DM particle is a fermion singlet under the gauge symmetries of the SM, which couples to a scalar boson which itself mixes with the Higgs. This model class provides a specific realization of the s-channel scalar mediator case discussed in Section 3. Its implications for the LHC have been studied for example in [62–65].
C. The DM particle itself may be a mixture of an electroweak singlet and doublet [66–68], as in the MSSM where it has both bino and higgsino components. Generically, this is referred to as "singlet–doublet" DM [69].

The first two cases capture important features of models [70,60,71] where the SM is extended to be classically scale invariant [72–75] with the aim of addressing the electroweak gauge hierarchy problem.

4.1. Scalar singlet DM

In the case where an additional real scalar singlet χ is the DM candidate, the Lagrangian of the scalar Higgs portal can be written as

$$\mathcal{L}_{\mathrm{scalar},H} \supset -\lambda_\chi \chi^4 - \lambda_p \chi^2 |H|^2, \tag{26}$$

where H denotes the usual SM Higgs doublet. Augmenting the Lagrangian with a discrete Z_2 symmetry that takes $\chi \to -\chi$ and $H \to H$ leads to stable DM, and in addition guarantees that there is no singlet-Higgs mixing, which leaves the couplings of the SM Higgs unaltered at tree level. The self-coupling λ_χ of the scalar χ is in general irrelevant to determining how well the portal coupling λ_p can be probed through LHC DM searches, and thus may be ignored.

For $m_h > 2m_\chi$, the most obvious manifestation of the interactions (26) is through their contributions to the invisible decay of the Higgs. The corresponding decay width reads

$$\Gamma(h \to \chi\chi) = \frac{\lambda_p^2 v^2}{2\pi m_h}\left(1 - \frac{4m_\chi^2}{m_h^2}\right)^{1/2}, \tag{27}$$

with m_h the Higgs mass and v its VEV. In fact, both ATLAS [76] and CMS [77] have already interpreted their Run I $h \to$ invisible searches in terms of the Higgs portal scenario (26). For DM candidates with $m_\chi \lesssim 10$ GeV these searches are competitive with or even stronger than the SI results provided by direct detection experiments.

When $m_h < 2m_\chi$, the Higgs cannot decay on-shell to a pair of χ particles, so that DM pair production necessarily has to proceed off-shell. The cross section for this process is then suppressed by an additional factor of λ_p^2 as well as the two-body phase space, leading to a rate that rapidly diminishes with m_χ. This feature makes a LHC discovery challenging even at 14 TeV and high luminosity [61].

4.2. Fermion singlet DM

A simple model including both a real scalar mediator s and a fermion DM singlet χ, which couple through a Higgs portal is given by

$$\mathcal{L}_{\mathrm{fermion},H} \supset -\mu_s s^3 - \lambda_s s^4 - y_\chi \bar\chi\chi s - \mu_p s|H|^2 - \lambda_p s^2|H|^2, \tag{28}$$

where y_χ is a Yukawa coupling in the dark sector, while the μ_p and λ_p terms provide the Higgs portal between the dark and the SM sectors. The precise values of the Higgs potential parameters μ_s and λ_s do not play an important role in the DM phenomenology at the LHC and therefore all features relevant for our discussion can be captured within the restricted framework $\mu_s = \lambda_s = 0$.

In general the Higgs potential in (28) develops non-trivial VEVs for both H and s, but in order to keep the expressions simple it is assumed in the following that $\langle s \rangle = 0$. The main physics implications are unaffected by this assumption. As a result of the portal coupling μ_p, the Higgs and the real scalar fields mix, giving rise to the physical mass eigenstates h_1 and h_2:

$$\begin{pmatrix} h_1 \\ h_2 \end{pmatrix} = \begin{pmatrix} \cos\theta & \sin\theta \\ -\sin\theta & \cos\theta \end{pmatrix} \begin{pmatrix} h \\ s \end{pmatrix}. \tag{29}$$

The mixing angle is defined such that in the limit $\theta \to 0$ the dark sector is decoupled from the SM. Analytically, one has

$$\tan(2\theta) = \frac{2v\mu_p}{m_s^2 + \lambda_p v^2 - m_h^2}, \tag{30}$$

while the masses of h_1 and h_2 are given by $m_{h_1} \simeq m_h$ and $m_{h_2} \simeq (m_s^2 + \lambda_p v^2)^{1/2}$. The state h_1 can therefore be identified with the bosonic resonance discovered at the LHC.

To make contact with the scalar mediator model described in Section 3, we consider the Yukawa terms that follow from (28). After electroweak symmetry breaking and rotation to the mass eigenstate basis, one finds

$$\begin{aligned} \mathcal{L} \supset & -\frac{1}{\sqrt{2}} (\cos\theta\, h_1 - \sin\theta\, h_2) \sum_f y_f \bar{f} f \\ & - (\sin\theta\, h_1 + \cos\theta\, h_2)\, y_\chi \bar{\chi}\chi . \end{aligned} \tag{31}$$

Identifying h_2 with the field ϕ in (11), one sees that as far as the couplings between h_2 and the SM fermions are concerned, the interactions (31) resemble those of the scalar mediator model described in Section 3 with $g_u = g_d = g_e = g_v = -\sin\theta$. The coupling between DM and the mediator, called g_χ in (11), is instead given by $g_\chi = y_\chi \cos\theta$.

Another important feature of (31) is that the effective Yukawa coupling between h_1 and the SM fermions is not y_f but $y_f \cos\theta$. In fact, the universal suppression factor $\cos\theta$ appears not only in the fermion couplings but also the $h_1 W^+W^-$ and $h_1 ZZ$ tree-level vertices as well as the loop-induced $h_1 gg$, $h_1\gamma\gamma$, and $h_1 \gamma Z$ couplings. The mixing angle and hence (28) is therefore subject to the constraints that arise from the ATLAS and CMS measurements of the signal strengths in Higgs production and decay. Global fits [78,79] to the LHC Run I data find $\sin\theta \lesssim 0.4$. Constraints on the mixing angle also derive from the oblique parameters T (*aka* the ρ parameter) and S [63], but they are typically weaker than those that follow from Higgs physics.

Like in the case of the scalar singlet DM model discussed before, the model (28) allows for invisible decays of the Higgs boson, if this is kinematically possible, i.e. $m_{h_1} > 2m_\chi$. The corresponding decay rate is

$$\Gamma(h_1 \to \chi\bar{\chi}) = \frac{y_\chi^2 \sin^2\theta\, m_{h_1}}{8\pi} \left(1 - \frac{4m_\chi^2}{m_{h_1}^2}\right)^{3/2}. \tag{32}$$

After the replacements $\sin\theta \to \cos\theta$ and $m_{h_1} \to m_{h_2}$ the same expression holds in the case of h_2, if it is sufficiently heavy. In order to determine from (32) the invisible Higgs branching ratio, one has to keep in mind that all partial widths of h_1 to SM particles are suppressed by $\cos^2\theta$ and that depending on the mass spectrum also the decay $h_1 \to h_2 h_2$ may be allowed.

Turning our attention to the $\not{E}_T$ signals, an important observation to make is that the phenomenology of the fermion singlet DM scenario is generically richer than that of the scalar mediator model (11). First of all, since the Lagrangian (28) leads to couplings between the scalars h_1 and h_2 to massive gauge bosons as well as DM pairs, mono-W and mono-Z signals will arise at tree level. The relevant diagrams are shown on the left-hand side in Fig. 4. The resulting amplitudes for mono-W or mono-Z production at the LHC take the following schematic form

$$\begin{aligned} \mathcal{A}(pp \to \not{E}_T + W/Z) \propto & \; y_\chi \sin(2\theta) \\ & \times \left(\frac{1}{s_{\chi\bar{\chi}} - m_{h_1}^2 + i m_{h_1}\Gamma_{h_1}} - \frac{1}{s_{\chi\bar{\chi}} - m_{h_2}^2 + i m_{h_2}\Gamma_{h_2}} \right), \end{aligned} \tag{33}$$

where $s_{\chi\bar{\chi}}$ denotes the invariant mass of the DM pair and Γ_{h_1} and Γ_{h_2} are the total decay widths of the scalars. Note that the contributions from virtual h_1/h_2 exchange have opposite sign in (33). This implies that the $\not{E}_T + W/Z$ signal cross sections can depend sensitively on m_{h_2} and m_χ as well as the cuts imposed in the analysis. The destructive interference between the contributions of the two scalar mediators is also at work for mono-jets and it is well-known [62–64] that it can be phenomenologically relevant in direct detection.

A second interesting consequence of (28) is that this Lagrangian gives rise to a mono-Higgs signal [65,80]. Two examples of Feynman graphs that provide a contribution are given on the right in Fig. 4. Notice that while a $\not{E}_T + h$ signal can also arise in the simplified s-channel scalar mediator scenario discussed in Section 3, the presence of the two scalar states h_1 and h_2 and the existence of trilinear Higgs vertices such as $h_1 h_2^2$ are likely to change the mono-Higgs phenomenology of (28) compared to (11).

4.3. Singlet–doublet DM

Singlet–doublet DM scenarios are the simplest example of models where the interactions between DM and the SM arise from mixing of a singlet with electroweak multiplets. A fermion singlet χ and a pair of fermion doublets with opposite hypercharge denoted by $\psi_1 = (\psi_1^0, \psi_1^-)^T$ and $\psi_2 = (\psi_2^+, \psi_2^0)^T$ are introduced. Assuming that the new fields are odd under a Z_2 symmetry under which the SM fields are even, the Lagrangian reads

$$\begin{aligned} \mathcal{L}_{\text{fermion,SD}} = & \; i\left(\bar{\chi}\partial\!\!\!/\chi + \bar{\psi}_1 D\!\!\!/\psi_1 + \bar{\psi}_2 D\!\!\!/\psi_2\right) - \frac{1}{2} m_S \chi^2 - m_D \psi_1\psi_2 \\ & - y_1 \chi H \psi_1 - y_2 \chi H^\dagger \psi_2 + \text{h.c.}, \end{aligned} \tag{34}$$

where D_μ denotes the covariant derivative. The model generalizes the bino–higgsino sector of the MSSM in the decoupling limit. In fact, the Yukawa couplings y_1 and y_2 are free parameters, whereas in the MSSM they are related to the $U(1)_Y$ gauge coupling.

After electroweak symmetry breaking, singlet and doublets mix. The physical spectrum consists of a pair of charged particles (χ^+, χ^-) with mass m_D and three neutral eigenstates defined by $(\chi_1, \chi_2, \chi_3)^T = U(\chi, \psi_1^0, \psi_2^0)^T$, where U is the unitary matrix that diagonalizes the mass matrix

$$\mathcal{M} = \begin{pmatrix} m_S & \frac{y_1 v}{\sqrt{2}} & \frac{y_2 v}{\sqrt{2}} \\ \frac{y_1 v}{\sqrt{2}} & 0 & m_D \\ \frac{y_2 v}{\sqrt{2}} & m_D & 0 \end{pmatrix}. \tag{35}$$

The DM candidate is the lightest eigenstate χ_1, whose composition in terms of gauge eigenstates is $\chi_1 = U_{11}\chi + U_{12}\psi_1^0 + U_{13}\psi_2^0$. In the singlet–doublet scenario, DM couples to the Higgs boson h and the SM gauge bosons through its doublet components. The induced interactions can be read off from

$$\mathcal{L} \supset -h\bar{\chi}_i (c^*_{h\chi_i\chi_j} P_L + c_{h\chi_i\chi_j} P_R)\chi_j - Z_\mu \bar{\chi}_i \gamma^\mu (c_{Z\chi_i\chi_j} P_L - c^*_{Z\chi_i\chi_j} P_R)\chi_j$$

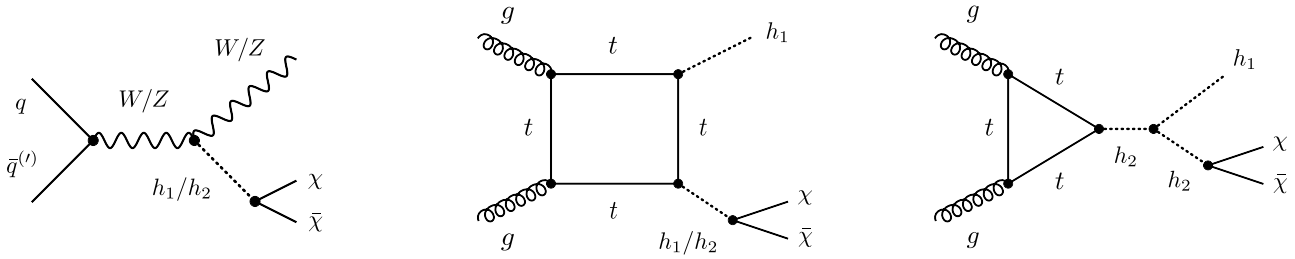

Fig. 4. Left: One-loop diagrams with an exchange of a h_1/h_2 mediator that induces a mono-W and mono-Z signal. Right: Two possible one-loop graphs that contribute to a mono-Higgs signal.

$$-\frac{g}{\sqrt{2}}(U_{i3}W^-_\mu\bar{\chi}_i\gamma^\mu P_L\chi^+ - U^*_{i2}W^-_\mu\bar{\chi}_i\gamma^\mu P_R\chi^+ + \text{h.c.}), \quad (36)$$

where $i, j = 1, 3$ and

$$\begin{aligned} c_{Z\chi_i\chi_j} &= \frac{g}{4\cos\theta_w}(U_{i3}U^*_{j3} - U_{i2}U^*_{j2}), \\ c_{h\chi_i\chi_j} &= \frac{1}{\sqrt{2}}(y_1U_{i2}U_{j1} + y_2U_{i3}U_{j1}), \end{aligned} \quad (37)$$

with g the $SU(2)_L$ coupling and $\cos\theta_w$ the cosine of the weak mixing angle. Due to these interactions, DM can annihilate to SM fermions via s-channel Higgs or Z-boson exchange and to bosons again through a Higgs or a Z boson in the s-channel or via χ_i or χ^+ in the t-channel. Likewise, Higgs (Z-boson) exchange leads to SI (SD) DM nucleon scattering. The corresponding phenomenology has been studied in [66,67,69,81].

As in the case of the other Higgs portal models, a possible collider signature is the invisible width of the Higgs, if the decay $h \to \chi_1\chi_1$ is kinematically allowed:

$$\Gamma(h \to \chi_1\chi_1) = \frac{m_h}{4\pi}\left(1 - \frac{4m^2_{\chi_1}}{m^2_h}\right)^{3/2}\left|c_{h\chi_1\chi_1}\right|^2. \quad (38)$$

Since the Z boson couples directly to pairs of DM particles χ_1, the model (34) will also give rise to an additional contribution to the invisible decay width of the Z boson of the form

$$\Gamma(Z \to \chi_1\chi_1) = \frac{m_Z}{6\pi}\left(1 - \frac{4m^2_{\chi_1}}{m^2_Z}\right)^{3/2}\left|c_{Z\chi_1\chi_1}\right|^2, \quad (39)$$

if $m_Z > 2m_{\chi_1}$. This possibility is constrained by the Z-pole measurements performed at LEP [82], which require $\Gamma(Z \to \chi_1\chi_1) \lesssim 3$ MeV.

Since the model (34) contains one charged and two neutral fermions in addition to the DM state χ_1, LHC searches for electroweak Drell–Yan production allow to set bounds on the new fermions arising in scalar-doublet scenarios. The relevant production modes are $q\bar{q} \to \chi_i\chi_j$ and $q\bar{q} \to \chi^+\chi^-$ via a Z boson or $q\bar{q}^{(\prime)} \to \chi^\pm\chi_i$ through W-boson exchange. Generically, the latter production mode has the most relevant LHC constraints. Production in gluon–gluon fusion $gg \to \chi_i\chi_i$ through an intermediate Higgs produced via a top-quark loop is also possible. Like in the case of electroweakino production in the MSSM, final states involving leptons and $\not{E}_T$ provide the cleanest way to probe singlet–doublet models [66,67,81]. A particularly promising channel is for instance $pp \to \chi^\pm\chi_{2,3} \to W^\pm\chi_1Z\chi_1$ that leads to both a $2\ell + \not{E}_T$ and $3\ell + \not{E}_T$ signature. The scenario (34) predicts further collider signals with $\not{E}_T$ such as mono-jets that await explorations.

5. Vector s-channel mediator

5.1. Model-building aspects

One of the simplest ways to add a new mediator to the SM is by extending its gauge symmetry by a new $U(1)'$, which is spontaneously broken such that the mediator obtains a mass M_V [83,84]. Depending on whether DM is a Dirac fermion χ or a complex scalar φ, the interactions this new spin-1 mediator take the form [18,85, 21,86–88]

$$\begin{aligned} \mathcal{L}_{\text{fermion},V} \supset\ & V_\mu\,\bar{\chi}\gamma^\mu(g^V_\chi - g^A_\chi\gamma_5)\chi \\ & + \sum_{f=q,\ell,\nu} V_\mu\bar{f}\gamma^\mu(g^V_f - g^A_f\gamma_5)f, \end{aligned} \quad (40)$$

$$\begin{aligned} \mathcal{L}_{\text{scalar},V} \supset\ & ig_\varphi V_\mu(\varphi^*\partial^\mu\varphi - \varphi\partial^\mu\varphi^*) \\ & + \sum_{f=q,\ell,\nu} V_\mu\bar{f}\gamma^\mu(g^V_f - g^A_f\gamma_5)f, \end{aligned} \quad (41)$$

where q, ℓ and ν denote all quarks, charged leptons and neutrinos, respectively. Under the MFV assumption the couplings of V to the SM fermions will be flavor independent, but they can depend on chirality (such that $g^A_f \neq 0$). For Majorana DM, the vector coupling g^V_χ vanishes, while a real scalar cannot have any CP-conserving interactions with V.

In the literature, one often finds a distinction between *vector* mediators with vanishing axialvector couplings ($g^A_f = 0$) and *axialvector* mediators with vanishing vector couplings ($g^V_f = 0$). Neglecting the couplings to neutrinos, the relevant parameters in the former case are

$$\left\{m_\chi,\ M_V,\ g^V_\chi,\ g^V_u,\ g^V_d,\ g^V_\ell\right\}, \quad (42)$$

while, in the latter case, the corresponding set is

$$\left\{m_\chi,\ M_V,\ g^A_\chi,\ g^A_u,\ g^A_d,\ g^A_\ell\right\}. \quad (43)$$

Note, however, that it is rather difficult to engineer purely axialvector couplings to all quarks, while being consistent with the SM Yukawa interactions and MFV (as explained below). In the following, we will consider the general case with non-zero vector and axialvector couplings. Although in this case the spin-1 mediator is not a parity eigenstate, we will refer to it as a vector mediator for simplicity.

5.1.1. The Higgs sector

The most straightforward way to generate the mass of the vector mediator is by introducing an additional dark Higgs field Φ with a non-zero VEV. Generically, this particle will not couple directly to SM fermions, but it could in principle mix with the SM Higgs, leading to a phenomenology similar to that of Higgs portal models described in Section 4. The mass of the dark Higgs cannot be very much heavier than that of the vector mediator, and so Φ may need to be included in the description if M_V is small compared to the typical energies of the collider.

Moreover, if the theory is chiral, i.e. if $g_\chi^A \neq 0$, the dark Higgs will also be responsible for generating the DM mass. In order for the Yukawa interaction $\Phi\bar{\chi}\chi$ to be gauge invariant, we have to require that the $U(1)'$ charge of the left-handed and the right-handed component of the DM field differ by exactly $q_L - q_R = q_\Phi$. Consequently, the axialvector coupling of DM to the mediator will necessarily be proportional to q_Φ. The longitudinal component of V (i.e. the would-be Goldstone mode) then couples to χ with a coupling strength proportional to $g_\chi^A m_\chi / M_V$. Requiring this interaction to remain perturbative gives the bound

$$m_\chi \lesssim \frac{\sqrt{4\pi}}{g_\chi^A} M_V, \tag{44}$$

implying that the DM mass cannot be raised arbitrarily compared to the mediator mass.

A similar consideration also applies in the visible sector. If the axialvector couplings to the SM states g_f^A are non-zero, the only way to have SM Yukawa couplings is if the SM Higgs doublet H carries a charge q_H under the new gauge group. This charge must satisfy $g' q_H = -g_u^A = g_d^A = g_e^A$ (where g' is the gauge coupling of the $U(1)'$) in order for quark and charged lepton masses to be consistent with the $U(1)'$ symmetry. However, having $q_H \neq 0$ generically implies corrections to electroweak precision measurements, so that one must require $M_V \gtrsim 2$ TeV for consistency with low-energy data.

5.1.2. Mixing with SM gauge bosons

As soon as there are fermions charged under both the SM gauge group and the new $U(1)'$, loop effects will induce mixing between the new vector mediator and the neutral SM gauge bosons, in particular kinetic mixing of the form

$$\mathcal{L}_{\text{kinetic}} \supset \frac{\epsilon}{2} F'^{\mu\nu} B_{\mu\nu}, \tag{45}$$

where $F'_{\mu\nu} = \partial_\mu V_\nu - \partial_\nu V_\mu$ and $B_{\mu\nu} = \partial_\mu B_\nu - \partial_\nu B_\mu$ denote the $U(1)'$ and $U(1)_Y$ field strength tensors. Parametrically, this mixing is given by

$$\epsilon \sim \sum_q \frac{(g_q^A)^2}{16\pi^2} \sim 10^{-2}\,(g_q^A)^2. \tag{46}$$

If M_V is too close to the Z-boson mass M_Z, this mixing can lead to conflicts with electroweak precision observables [89,84,90,91]. For example, the correction to the ρ parameter, $\Delta\rho = M_W^2/(M_Z^2\cos^2\theta_w) - 1$, can be estimated to be

$$\Delta\rho \sim \epsilon^2 \frac{M_Z^2}{M_V^2 - M_Z^2}. \tag{47}$$

Requiring $\Delta\rho \lesssim 10^{-3}$ [92] then implies $g_q^A \lesssim 1$ and $M_V \gtrsim 100$ GeV.

5.2. Phenomenological aspects

The first observation is that in models with s-channels mediators, the possibility for such particles to decay back to the SM is unavoidably present. This can show up as di-jets [86] or di-leptons at the LHC. Indeed the leptonic couplings g_ℓ^V and g_ℓ^A are very tightly constrained by searches for di-lepton resonances [87,88]. If the quark couplings of the mediator are equally small, it becomes very difficult to have sizable interactions between the SM and DM and there would typically be no observable DM signals. We therefore focus on the case where the quark couplings of the vector mediator are much larger than the lepton couplings, for example because the SM quarks are charged under the new $U(1)'$ while couplings to leptons only arise at loop-level (a so-called *leptophobic* Z' boson).

For such a set-up to be theoretically consistent we must require additional fermions charged under the $U(1)'$ and the SM gauge group to cancel anomalies. The masses of these additional fermions are expected to be roughly of the order of M_V, so they can often be neglected in phenomenology, unless the mass of the vector mediator is taken to be small compared to the typical energy scales of the collider. Indeed, it is possible to construct anomaly-free models with no direct couplings to leptons (for example in the context of a baryonic Z' boson [93,94]). In this case, the leptonic couplings will not give a relevant contribution to the DM phenomenology of the model and one can simply set $g_\ell^V = g_\ell^A = 0$.

5.2.1. Collider searches

If the vector mediator is kinematically accessible at the LHC, the resulting phenomenology depends crucially on its decay pattern. For arbitrary vector and axialvector couplings, one finds in the case of Dirac DM the following expression for the total width:

$$\Gamma_V = \frac{M_V}{12\pi} \sum_{i=f,\chi} N_c^i \left(1 - \frac{4m_i^2}{M_V^2}\right)^{1/2} \times \left[(g_i^V)^2 + (g_i^A)^2 + \frac{m_i^2}{M_V^2}\left(2(g_i^V)^2 - 4(g_i^A)^2\right)\right]. \tag{48}$$

Here the sum extends over all fermions i that are above threshold, while $N_c^i = 3$ for quarks and $N_c^i = 1$ for leptons and DM.

There are several important conclusions that can be drawn from (48). The first one concerns the maximal size that the couplings can take to be consistent with $\Gamma_V/M_V < 1$, which is a necessary requirement in order for a perturbative description of the mediator to be valid. Assuming that $M_V \gg m_i$ and setting for simplicity $g_q^V = g_\chi^V = g$ and $g_\ell^V = g_i^A = 0$, one finds that $\Gamma_V/M_V \simeq 0.5 g^2$. This implies that one has to have $g \lesssim 1.4$ in order for the width of the mediator to be smaller than its mass and values of g significantly below unity for the NWA (which calls for $\Gamma_V/M_V \lesssim 0.25$) to be applicable.

In cases where the NWA can be used, production and decay factorize such that for instance $\sigma(pp \to Z + \chi\bar{\chi}) = \sigma(pp \to Z + V) \times \text{Br}(V \to \chi\bar{\chi})$. The resulting LHC phenomenology is thus determined to first approximation by the leading decay mode of the vector mediator. Considering a situation with $M_V \gg m_i$ and $g_\ell^V = g_i^A = 0$, one finds that decays into quarks dominate if $g_\chi^V/g_q^V \lesssim 4$, while invisible decays dominate if $g_\chi^V/g_q^V \gtrsim 4$. For $g_\chi^V/g_q^V \simeq 4$ both decay channels have comparable branching ratios. If invisible decays dominate, the strongest collider constraints are expected from searches for $\not{E}_T$ in association with SM particles. To illustrate this case, we discuss mono-jet searches below. If, on the other hand, the invisible branching ratio is small, we expect most of the mediators produced at the LHC to decay back into SM particles. In this case, strong constraints can be expected from searches for heavy resonances, and we focus on di-jet resonances.

Mono-Jets

LHC searches for $\not{E}_T$ plus jet signals place strong constraints on the interactions between quarks and DM mediated by a vector mediator [20,21,14,95,40,96–98]. The corresponding cross sections can be calculated at next-to-leading order (NLO) in `MCFM` [38] and at NLO plus parton shower in the `POWHEG BOX` [46]. Some of the relevant diagrams are shown in Fig. 5. If the mediator is too heavy to be produced on-shell at the LHC and assuming equal vector couplings of the mediator to all quarks as well as $g_\ell^V = g_i^A = 0$, the mono-jet cross section at the LHC is proportional to $(g_q^V)^2\,(g_\chi^V)^2$. The same scaling applies if the mediator is forced

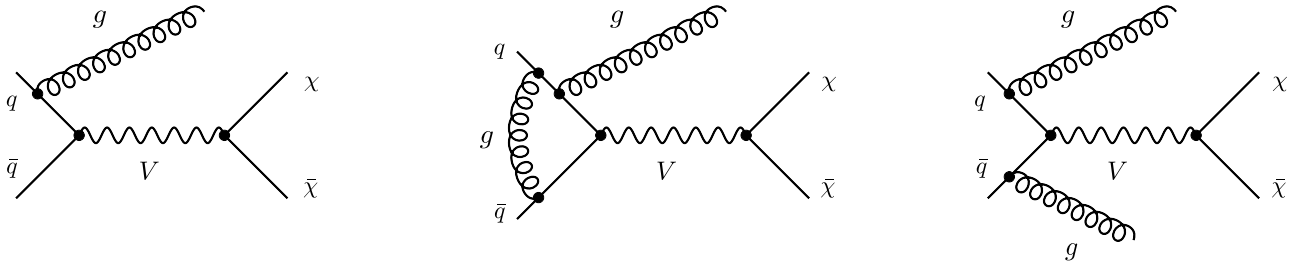

Fig. 5. Left: An example of a LO diagram that leads to mono-jet events through the s-channel exchange of a spin-1 vector resonance V. Right: At the NLO level both virtual and real corrections have to taken into account in order to obtain a infrared finite result.

to be off-shell because $M_V < 2m_\chi$ so that decays into DM are kinematically forbidden.

For $2m_\chi \ll M_V \ll \sqrt{s}$, with $\sqrt{s}$ the center-of-mass of the collider, the mediator can be produced on-shell and subsequently decay into a pair of DM particles. If the mediator width is small enough for the NWA to be valid, the mono-jet cross section will be proportional to the product $(g_q^V)^2\,\mathrm{Br}(V \to \chi\bar{\chi})$. If we fix the ratio g_χ^V/g_q^V, the invisible branching ratio will be independent of an overall rescaling of the couplings, so that we simply obtain $\sigma(pp \to \not{E}_T + j) \propto (g_q^V)^2$. If we rescale only one of the couplings, on the other hand, the resulting change in the mono-jet cross section will depend on the dominant decay channels of the mediator. If the total width of the mediator is dominated by its decays into quarks, the mono-jet cross section will be invariant under a rescaling of the quark coupling g_q^V, because the change in the production cross section is compensated by the change in the invisible branching ratio. If, on the other hand, invisible decays dominate, both the production cross section and the invisible branching ratio will be invariant under a (small) change in the coupling g_χ^V.

The same general considerations apply for axialvector couplings instead of vector couplings. In particular, the production cross section of the vector mediator is largely invariant under the exchange $g_q^V \leftrightarrow g_q^A$. Note, however, that for $m_\chi \to M_V/2$ the phase space suppression is stronger for axialvector couplings than for vector couplings, such that for $m_\chi \simeq M_V/2$ the mono-jet cross section is somewhat suppressed for a mediator with purely axialvector couplings.

In many situations invisible decays and decays into quarks will both lead to a non-negligible contribution to Γ_V as given in (48) and furthermore this width may become so large that one cannot use the NWA to derive simple scaling laws. If m_χ becomes close to $M_V/2$ there can also be contributions from both on-shell and off-shell mediators. As a result, all relevant parameters (m_χ, M_V, g_χ^V and g_q^V) must in general be taken into account in order to calculate mono-jet cross sections.

Di-Jets

Searches for di-jet resonances exploit the fact that any mediator produced from quarks in the initial state can also decay back into quarks, which lead to observable features in the distribution of the di-jet invariant mass and their angular correlations. However, for small mediator masses the QCD background resulting from processes involving gluons in the initial state completely overwhelms the signal. The most recent di-jet searches at the LHC therefore focus mostly on the region with di-jet invariant mass $m_{jj} \gtrsim 1$ TeV. For smaller mediator masses, the strongest bounds are in fact obtained from searches for di-jet resonances at UA2 and the Tevatron [98]. An interesting opportunity to make progress with the LHC even in the low-mass region is to consider the production of di-jet resonances in association with other SM particles, such as W or Z bosons, which suffer from a significantly smaller QCD background [99,100].

An important complication concerning searches for di-jet resonances results from the fact that the width of the mediator can be fairly large. The steeply falling parton distribution functions then imply that the resonance will likely be produced at lower masses, leading to a significant distortion of the expected distribution of invariant masses m_{jj}. Existing searches for narrow resonances therefore typically do not apply to vector mediators with couplings of order unity. Nevertheless, the shape of the resonance can still be distinguished from SM backgrounds and it is still possible to constrain these models using specifically designed searches [98].

A number of such searches have been considered in [98]. The central conclusion is that, at least for $g_q^V \lesssim 1$, bounds on M_V become stronger as g_q^V is increased, because the enhancement of the production cross section is larger than the reduction of the detection efficiency resulting from the increasing width. Indeed, there are still stringent bounds on mediators with width as large as $\Gamma_V \sim M_V/2$. It is *crucial* to take these bounds into account when interpreting DM searches at the LHC in terms of simplified models with an s-channel vector mediator, because they apply to a wide range of models and in many cases complement or even surpass other search strategies. A promising strategy to constrain even broader resonances may be to study di-jet angular correlations, such as the ones considered in the context of constraining four-fermion operators (see for instance [101,102]).

5.2.2. Direct detection

Depending on the coupling structure of the vector mediator, the interactions of DM with nuclei can proceed via SI or SD scattering off nucleons. The corresponding cross sections at zero-momentum transfer are given by

$$\sigma^{\mathrm{SI}}_{\chi-N} = \frac{\mu^2_{\chi-N}}{\pi M_V^4} f_N^2, \qquad \sigma^{\mathrm{SD}}_{\chi-N} = \frac{3\mu^2_{\chi-N}}{\pi M_V^4}\, a_N^2, \tag{49}$$

where N stands for either p or n, while f_N and a_N denote the effective nucleon couplings. They take the form

$$f_p = g_\chi^V(2g_u^V + g_d^V), \qquad f_n = g_\chi^V(g_u^V + 2g_d^V), \tag{50}$$

and

$$a_{p,n} = g_\chi^A \sum_{q=u,d,s} \Delta q^{(p,n)}\, g_q^A. \tag{51}$$

The coefficients $\Delta q^{(N)}$ encode the contributions of the light quarks to the nucleon spin. They are given by [92]

$$\begin{aligned} \Delta u^{(p)} &= \Delta d^{(n)} = 0.84 \pm 0.02, \\ \Delta d^{(p)} &= \Delta u^{(n)} = -0.43 \pm 0.02, \\ \Delta s^{(p)} &= \Delta s^{(n)} = -0.09 \pm 0.02. \end{aligned} \tag{52}$$

Potential cross terms such as $g_q^V g_\chi^A$ are suppressed in the non-relativistic limit (either by the momentum transfer or the DM

velocity, both of which lead to a suppression of 10^{-3} or more), and can therefore be neglected.

Substituting the expressions for the effective couplings into the formulas for the DM-nucleon scattering cross sections, we obtain

$$\sigma^{\rm SI}_{\chi-N} = 1.4\times10^{-37}\ {\rm cm}^2\, g^V_\chi g^V_q \left(\frac{\mu_{\chi-N}}{1\ {\rm GeV}}\right)^2 \left(\frac{300\ {\rm GeV}}{M_V}\right)^4, \quad (53)$$

$$\sigma^{\rm SD}_{\chi-N} = 4.7\times10^{-39}\ {\rm cm}^2\, g^A_\chi g^A_q \left(\frac{\mu_{\chi-N}}{1\ {\rm GeV}}\right)^2 \left(\frac{300\ {\rm GeV}}{M_V}\right)^4. \quad (54)$$

Crucially, SI interactions receive a coherent enhancement proportional to the square of the target nucleus mass, leading to very strong constraints from direct detection experiments unless the DM mass is very small. Consequently, the estimates above imply that for $g_q \simeq 1$, SI interactions are sensitive to mediator masses of up to $M_V \simeq 30$ TeV, while SD interactions only probe mediator masses up to around $M_V \simeq 700$ GeV. This should be contrasted with the constraints arising from the LHC, which are close to identical for vector and axialvector mediators.

5.2.3. Annihilation

Two processes contribute to DM annihilation in the early Universe: annihilation of DM into SM fermions and (provided $M_V \lesssim m_\chi$) direct annihilation into pairs of mediators, which subsequently decay into SM states. For the first process, the annihilation cross section is given by

$$\begin{aligned}(\sigma v)(\chi\bar\chi\to V\to q\bar q) &= \frac{3m_\chi^2}{2\pi\left[(M_V^2-4m_\chi^2)^2+\Gamma_V^2M_V^2\right]}\left(1-\frac{4m_q^2}{M_V^2}\right)^{1/2}\\ &\times\left\{(g^V_\chi)^2\left[(g^V_q)^2\left(2+\frac{m_q^2}{M_V^2}\right)+2\,(g^A_q)^2\left(1-\frac{m_q^2}{M_V^2}\right)\right]\right.\\ &\left.+(g^A_q)^2(g^A_\chi)^2\frac{m_q^2}{M_V^2}\frac{(4m_\chi^2-M_V^2)^2}{M_V^4}\right\}, \end{aligned} \quad (55)$$

where Γ_V is the total decay width of the vector mediator as given in (48). For $m_\chi \simeq M_V/2$ the annihilation rate receives a resonant enhancement, leading to a very efficient depletion of DM.

An important observation is that for $g^V_\chi = 0$, the annihilation cross section is helicity-suppressed. For $m_b \ll m_\chi < m_t$ the factor m_q^2/m_χ^2 can be very small, such that it is important to also include the p-wave contribution for calculating the DM relic abundance. Including terms up to second order in the DM velocity v, we obtain for the special case $g^V_q = g^V_\chi = 0$ the expression

$$\begin{aligned}(\sigma v)(\chi\bar\chi\to V\to q\bar q) &= \frac{(g^A_q)^2(g^A_\chi)^2\,m_\chi^2}{2\pi\left[(M_V^2-4m_\chi^2)^2+\Gamma_V^2M_V^2\right]}\left(1-\frac{4m_q^2}{M_V^2}\right)^{1/2}\\ &\times\left\{\frac{3m_q^2}{M_V^2}\frac{(4m_\chi^2-M_V^2)^2}{M_V^4}+\left(1-\frac{m_q^2}{M_V^2}\right)v^2\right\}. \end{aligned} \quad (56)$$

Finally, the annihilation cross section for direct annihilation into pairs of mediators is given by

$$\begin{aligned}(\sigma v)(\chi\bar\chi\to VV) &= \frac{(m_\chi^2-M_V^2)^{3/2}}{4\pi\, m_\chi M_V^2(M_V^2-2m_\chi^2)^2}\\ &\times\left(8(g^A_\chi)^2(g^V_\chi)^2m_\chi^2+\left[(g^A_\chi)^4-6(g^A_\chi)^2(g^V_\chi)^2+(g^V_\chi)^4\right]M_V^2\right). \end{aligned} \quad (57)$$

We note that for the coupling strengths and mass ranges typically considered in the context of LHC DM searches, it is easily possible to achieve sufficiently large annihilation cross sections to deplete the DM abundance in the early Universe. In fact, the generic prediction in large regions of parameter space would be that the DM particle is underproduced. In this case, the observed DM relic abundance can still be reproduced if one assumes an initial particle–antiparticle asymmetry in the dark sector, such that only the symmetric component annihilates away and the final DM abundance is set by the initial asymmetry.

6. t-channel flavored mediator

If the DM is a fermion χ, the mediator can be a colored scalar or a vector particle ϕ. We focus on the scalar case, which makes contact with the MSSM and is easier to embed into a UV-complete theory. A coupling of the form $\phi\bar\chi q$ requires either χ or ϕ to carry a flavor index in order to be consistent with MFV. We choose the case where the colored scalar ϕ carries the flavor index (much like in the MSSM case, where the colored scalar quarks come in the same flavors as the SM quarks). This class of models has been considered previously in [103–108,16], while models where χ carries the flavor index have been studied in [109–111].

There are variations where the mediator couples to right-handed up-type quarks, right-handed down-type quarks, or left-handed quark doublets. For definiteness, we discuss the right-handed up-type case (the other cases are obtained in a similar fashion). In this case, there are three mediators $\phi_i = \{\tilde u, \tilde c, \tilde t\}$, which couple to the SM and DM via the interaction

$$\mathcal{L}_{{\rm fermion},\tilde u} \supset \sum_{i=1,2,3} g\phi_i^*\,\bar\chi P_R u_i + {\rm h.c.} \quad (58)$$

Note that MFV requires both the masses $M_{1,2,3}$ of the three mediators to be equal and universal couplings $g = g_{1,2,3}$ between the mediators and their corresponding quarks $u_i = \{u, c, t\}$. This universality can however be broken by allowing for corrections to (58) and the mediator masses which involve a single insertion of the flavor spurion $Y^{u\dagger}Y^u$. Because of the large top-quark Yukawa coupling, in this way the mass of the third mediator and its coupling can be split from the other two. In practice this means that the generic parameter space is five-dimensional:

$$\left\{m_\chi,\ M_{1,2},\ M_3,\ g_{1,2},\ g_3\right\}. \quad (59)$$

These simplified models are very similar to the existing ones for squark searches [112], and results can often be translated from one to the other with relatively little work. Note that most studies will involve $g_{1,2}$ together with $M_{1,2}$ *or* g_3 together with M_3. So specific applications will often have a smaller dimensional space of relevant parameters. In the discussion below, we restrict attention to the parameter space with $g_{1,2}$, $M_{1,2}$, and m_χ. For models where g_3 and M_3 are relevant, see [113,114,111,115].

6.1. Collider constraints

Given the masses and couplings, the widths of the mediators are calculable. One finds

$$\begin{aligned}\Gamma(\phi_i\to\chi\bar u_i) &= \frac{g_i^2}{16\pi M_i^3}(M_i^2-m_{u_i}^2-m_\chi^2)\\ &\times\sqrt{M_i^4+m_{u_i}^4+m_\chi^4-2M_i^2m_{u_i}^2-2M_i^2m_\chi^2-2m_\chi^2m_{u_i}^2}\\ &= \begin{cases}\dfrac{g_i^2}{16\pi}M_i\left(1-\dfrac{m_\chi^2}{M_i^2}\right)^2, & M_i, m_\chi \gg m_{u_i}.\\ \dfrac{g_i^2}{16\pi}M_i, & M_i \gg m_\chi, m_{u_i}.\end{cases}\end{aligned} \quad (60)$$

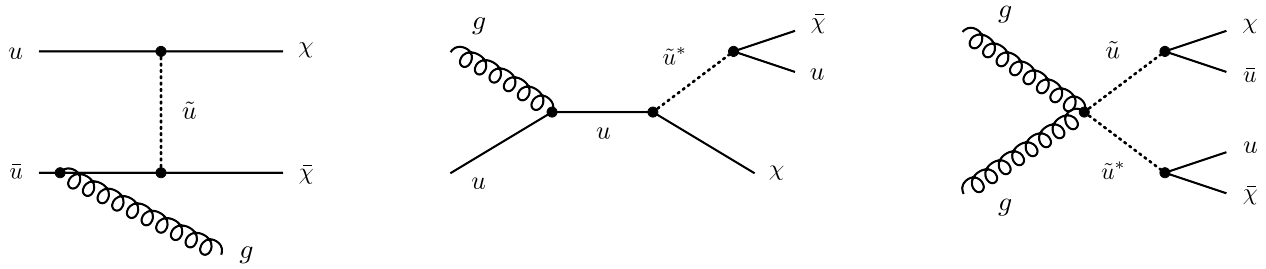

Fig. 6. A $\not{E}_T + j$ signal can arise in the t-channel mediator scenario from initial-state gluon emission (left) and associated mediator production (middle). Initial-state gluon splitting processes and gluon emission from the t-channel mediator is also possible but not shown. Pair production of the mediator $\tilde{u}$ in gluon fusion leads instead to $\not{E}_T + 2j$ events (right). Quark-fusion pair production either via s-channel gluon or t-channel DM exchange also contributes to the latter signal.

Unless the final-state quark u_i is a top quark, the given limiting cases are always very good approximations to the exact widths.

In the context of (58) the production channels that lead to a $\not{E}_T + j$ signal are $u\bar{u} \to \chi\bar{\chi} + g$, $ug \to \chi\bar{\chi} + u$ and $\bar{u}g \to \chi\bar{\chi} + \bar{u}$. Examples of the relevant Feynman diagrams are shown on the left and in the middle of Fig. 6. In addition, if the colored mediator $\tilde{u}$ is sufficiently light it may be pair produced from both gg or $u\bar{u}$ initial states. This gives rise to a $\not{E}_T + 2j$ signature as illustrated by the graph on the right-hand side in the same figure. If the DM particle is a Majorana fermion also the uu and $\bar{u}\bar{u}$ initial states contribute to the production of mediator pairs. The latter corrections vanish if χ is a Dirac fermion. From this brief discussion, it should be clear that t-channel models can be effectively probed through both mono-jet and squark searches.

6.1.1. Mono-Jet searches

Given that in all recent mono-jet analyses a second hard jet is allowed, the corresponding LHC searches are sensitive in t-channel models to the contributions not only from initial-state gluon radiation and associated production, but also to mediator pair production. Since the relative importance of the different channels depends on m_χ, M_1, and g_1 as well as the imposed experimental cuts, all corrections should be included in an actual analysis. General statements about the leading partonic channel are however possible. For what concerns $\not{E}_T + j$ events the diagram in the middle of Fig. 6 usually gives the dominant contribution. Compared to $u\bar{u} \to \chi\bar{\chi} + g$, this process benefits from a phase-space enhancement, the larger gluon luminosity, and the fact that jets from initial state radiation tend to be softer. If the mass M_1 is small, diagrams with gluon emission from the mediator can also be important, but these graphs are subdominant if the mediator is heavy, since they are $1/M_1^2$ suppressed. Notice that the dominance of the associated production channel is a distinct feature of t-channel models that is not present in the case of s-channel mediators, nor is it relevant in supersymmetric theories where the mediator is a squark. The relative importances of the different $\not{E}_T + j$ and $\not{E}_T + 2j$ channels depend sensitively on how g_1 compares to the strong coupling constant g_s. In the limit $g_1 \ll g_s$, pure QCD pair production dominates, while in the opposite case graphs with DM exchange are more important. Detailed studies of the bounds on the coupling g_1 as a function of M_1 and m_χ that arise from Run I mono-jet data have been presented in [106,108].

6.1.2. Squark searches

If the t-channel mediator is light it can be copiously produced in pairs at the LHC and then decay into DM and a quark. The resulting phenomenology is very similar to squark pair production in the MSSM with a decoupled gluino. There is however one important difference which has to do with the fact that in supersymmetric theories the coupling between the squarks and the neutralino χ is necessarily weak. The cross section for squark pair production through t-channel exchange of DM is therefore negligible. This is not the case in t-channel mediator scenarios, because g_1 is a free parameter and thus it is possible to enhance significantly the $\tilde{u}$ pair production rate associated to t-channel DM exchange. As already mentioned, the quark-fusion pair production cross section depends on whether χ is a Dirac or a Majorana particle. In the former case only $u\bar{u}$-initiated production is non-zero, while in the latter case also the uu and $\bar{u}\bar{u}$ initial states furnish a contribution. The constraints from LHC squark searches on t-channel mediator models with both Dirac and Majorana DM have been investigated thoroughly in [104,106–108]. These studies show that squark and mono-jet searches provide comparable and complementary bounds on a wide range of the parameter space of t-channel scenarios, depending on the masses of the mediator and DM. Especially in the case where the DM particle and the mediator are quasi-degenerate in mass, mono-jet searches turn out to be superior.

6.2. Scattering with nucleons

Away from resonance and neglecting light quark-mass effects, the SI scattering cross section of Dirac DM and nucleons that is induced by (58) reads

$$\sigma^{\rm SI}_{\chi-N} = \frac{g_1^4 \mu^2_{\chi-N}}{64\pi \left(M_1^2 - m_\chi^2\right)^2} f_N^2. \tag{61}$$

Here $f_p = 2$ and $f_n = 1$ and hence the SI cross sections for protons and neutrons are different in the t-channel scenario. Using the same approximations the subleading SD scattering cross section takes the form

$$\sigma^{\rm SD}_{\chi-N} = \frac{3 g_1^4 \mu^2_{\chi-N}}{64\pi \left(M_1^2 - m_\chi^2\right)^2} \left(\Delta u^{(N)}\right)^2, \tag{62}$$

with the numerical values for $\Delta u^{(N)}$ given in (52). Notice that for Majorana DM, the SI scattering cross section vanishes and the expression for $\sigma^{\rm SD}_{\chi-N}$ is simply obtained from (62) by multiplying the above result by a factor of 4.

Since in t-channel models with Dirac DM one has $\sigma^{\rm SI}_{\chi-N} \neq 0$, the existing direct detection constraints dominate over the collider bounds up to very low DM masses of around 5 GeV. For Majorana DM instead – as a result of the lack of the enhancement from coherence in DM-nucleus scattering – the LHC constraints turn out to be stronger than the direct detection limits for DM masses up to of a few hundred GeV.

6.3. Annihilation rates

The main annihilation channel of DM in the framework of (58) is $\chi\bar{\chi} \to u_i\bar{u}_i$. In the Dirac case this leads to a s-wave contribution of the form

$$(\sigma v)(\chi\bar{\chi} \to u_i\bar{u}_i) = \frac{3 g_i^4 m_\chi^2}{32\pi \left(M_i^2 + m_\chi^2\right)^2}, \tag{63}$$

if quark masses are neglected (remember that an additional factor of 1/2 has to be included in the thermal averaging). In the Majorana case, annihilation to SM quarks is instead p-wave suppressed and given for zero quark masses by

$$(\sigma v)(\chi\chi \to u_i\bar{u}_i) = \frac{g_i^4 m_\chi^2 (M_i^4 + m_\chi^4)}{16\pi \left(M_i^2 + m_\chi^2\right)^4} v^2. \tag{64}$$

In the parameter space where the mediator ϕ_i and the DM particle χ are quasi-degenerate in mass and the ratio $(M_i - m_\chi)/m_\chi$ is comparable to or below the freeze-out temperature, co-annihilation effects become important [116,117]. For both Dirac and Majorana fermions the annihilation cross section for $\chi\phi_i \to u_i g$ can be written as

$$(\sigma v)(\chi\phi_i^* \to u_i g) = \frac{g_s^2 g_i^2}{24\pi M_i \left(M_i + m_\chi\right)}, \tag{65}$$

if quark-mass effects and v^2-suppressed terms are neglected. In addition the mediators ϕ_i can self-annihilate. While for both Dirac and Majorana DM annihilation to gluons

$$(\sigma v)(\phi_i\phi_i^* \to gg) = \frac{7 g_s^4}{216\pi M_i^2}, \tag{66}$$

proceeds via s-wave, the process $\phi_i\phi_i^* \to u_i\bar{u}_i$ is p-wave suppressed and hence subdominant. Finally, for Majorana DM the reaction $\phi_i\phi_i \to u_i u_i$ (and its charge conjugate) is possible. The relevant s-wave contribution in this case reads

$$(\sigma v)(\phi_i\phi_i \to u_i u_i) = \frac{g_i^4 m_\chi^2}{6\pi \left(M_i^2 + m_\chi^2\right)^2}. \tag{67}$$

Assuming that the relic abundance $\Omega_\chi h^2$ is thermally produced, one finds that for Dirac DM there is no region in the parameter space that satisfies the combined constraints arising from the LHC searches, direct detection, and $\Omega_\chi h^2$. Therefore the simple model (58) with Dirac DM cannot be regarded as a complete model in describing the interactions between the dark and the visible sectors. In the case of Majorana fermions satisfying all three requirements is possible, but the mass of DM must be larger than about 100 GeV. If DM is lighter there must be other channels for DM to annihilate into, which calls for additional new physics.

7. Conclusions

The primary goal of this document is to outline a set of simplified models of DM and their interactions with the SM. It can thus serve as a summary and proposal for the simplified models to be implemented in future searches for DM at the LHC. The list of models discussed includes spin-0 and spin-1 s-channel mediator scenarios as well as t-channel models. The most important prototypes of Higgs-portal scenarios are also described. To motivate our choice of simplified models, a number of guiding principles have been given that theories of DM–SM interactions should satisfy in order to be useful at LHC energies (and possibly beyond). Based on these criteria building further simplified (or even complete) DM models is possible. While the focus is on giving a brief account of the LHC signals that seem most relevant in each of the simplified models, we have also provided expressions and formulas for reference that allow the reader to derive the constraints from direct and indirect searches for DM. There is still useful work to be done to improve our understanding of simplified DM models, and room to devise creative new searches that can discover or constrain them.

While most of the discussion in this work centers around simplified models, we emphasize that the given examples represent only "theoretical sketches" of DM–SM interactions, and that they by no means exhaust the whole spectrum of possibilities that the DM theory space has to offer. They are neither meant to form self-contained, complete pictures of DM interactions at the LHC, nor are they meant to be model-independent and general enough to cover the *entirety* of the DM landscape. In order to do justice to the range of options in the DM theory space, it is thus important when searching for DM at the LHC to frame the results of searches in terms of all three types of theoretical frameworks: EFTs, simplified models, and UV complete theories. Only in this way is it possible to maximize the search coverage for DM at LHC Run II, and have the largest possible impact on our understanding of the particle properties of DM. Simplified models thus play a crucial role in this endeavor.

Acknowledgments

The DM@LHC2014 Workshop organizers wish to acknowledge the generous support of the UK's Science and Technology Facilities Council, the Rutherford Appleton Laboratory, the University of Oxford, Imperial College London, IPPP Durham, the Université de Genève, and Dark Matter Coffee of Chicago. The final session of the workshop, a discussion session highlighting simplified models, was supported by the Institute of Physics as a "Half-Day Meeting". In addition we gratefully acknowledge support for staff provided by CERN and the following funding agencies: ARC (Australia); FNRS and FWO (Belgium); NSERC, NRC, and CFI (Canada); CAS, MoST and NSFC (China); CEA and CNRS/IN2P3 (France); BMBF, DFG, HGF and MPG (Germany); INFN (Italy); ISF (Israel); MEXT and JSPS (Japan); MOE and UM (Malaysia); FOM and NWO (The Netherlands); SNSF and SER (Switzerland); MST (Taiwan); STFC (United Kingdom); DOE and NSF (USA).

References

[1] G. Bertone, D. Hooper, J. Silk, Phys. Rep. 405 (2005) 279. [hep-ph/0404175].
[2] A. Askew, S. Chauhan, B. Penning, W. Shepherd, M. Tripathi, Internat. J. Modern Phys. A 29 (2014) 1430041. arXiv:1406.5662 [hep-ph].
[3] Q.H. Cao, C.R. Chen, C.S. Li, H. Zhang, J. High Energy Phys. 1108 (2011) 018. arXiv:0912.4511 [hep-ph].
[4] M. Beltran, D. Hooper, E.W. Kolb, Z.A.C. Krusberg, T.M.P. Tait, J. High Energy Phys. 1009 (2010) 037. arXiv:1002.4137 [hep-ph].
[5] J. Goodman, M. Ibe, A. Rajaraman, W. Shepherd, T.M.P. Tait, H.B. Yu, Phys. Lett. B 695 (2011) 185. arXiv:1005.1286 [hep-ph].
[6] Y. Bai, P.J. Fox, R. Harnik, J. High Energy Phys. 1012 (2010) 048. arXiv:1005.3797 [hep-ph].
[7] J. Goodman, M. Ibe, A. Rajaraman, W. Shepherd, T.M.P. Tait, H.B. Yu, Phys. Rev. D 82 (2010) 116010. arXiv:1008.1783 [hep-ph].
[8] J. Goodman, M. Ibe, A. Rajaraman, W. Shepherd, T.M.P. Tait, H.B. Yu, Nuclear Phys. B 844 (2011) 55. arXiv:1009.0008 [hep-ph].
[9] A. Rajaraman, W. Shepherd, T.M.P. Tait, A.M. Wijangco, Phys. Rev. D 84 (2011) 095013. arXiv:1108.1196 [hep-ph].
[10] P.J. Fox, R. Harnik, J. Kopp, Y. Tsai, Phys. Rev. D 85 (2012) 056011. arXiv:1109.4398 [hep-ph].
[11] P.J. Fox, R. Harnik, J. Kopp, Y. Tsai, Phys. Rev. D 84 (2011) 014028. arXiv:1103.0240 [hep-ph].
[12] I.M. Shoemaker, L. Vecchi, Phys. Rev. D 86 (2012) 015023. arXiv:1112.5457 [hep-ph].
[13] G. Busoni, A. De Simone, E. Morgante, A. Riotto, Phys. Lett. B 728 (2014) 412. arXiv:1307.2253 [hep-ph].
[14] O. Buchmueller, M.J. Dolan, C. McCabe, J. High Energy Phys. 1401 (2014) 025. arXiv:1308.6799 [hep-ph].
[15] G. Busoni, A. De Simone, J. Gramling, E. Morgante, A. Riotto, J. Cosmol. Astropart. Phys. 060 (2014) arXiv:1402.1275 [hep-ph].
[16] G. Busoni, A. De Simone, T. Jacques, E. Morgante, A. Riotto, J. Cosmol. Astropart. Phys. 1409 (2014) 022. arXiv:1405.3101 [hep-ph].
[17] D. Racco, A. Wulzer, F. Zwirner, J. High Energy Phys. 1505 (2015) 009. arXiv:1502.04701 [hep-ph].
[18] E. Dudas, Y. Mambrini, S. Pokorski, A. Romagnoni, J. High Energy Phys. 0908 (2009) 014. arXiv:0904.1745 [hep-ph].
[19] J. Goodman, W. Shepherd, arXiv:1111.2359 [hep-ph].
[20] H. An, X. Ji, L.T. Wang, J. High Energy Phys. 1207 (2012) 182. arXiv:1202.2894 [hep-ph].
[21] M.T. Frandsen, F. Kahlhoefer, A. Preston, S. Sarkar, K. Schmidt-Hoberg, J. High Energy Phys. 1207 (2012) 123. arXiv:1204.3839 [hep-ph].
[22] H. Dreiner, D. Schmeier, J. Tattersall, Europhys. Lett. 102 (2013) 51001. arXiv:1303.3348 [hep-ph].

[23] R.C. Cotta, A. Rajaraman, T.M.P. Tait, A.M. Wijangco, Phys. Rev. D 90 (2014) 013020. arXiv:1305.6609 [hep-ph].
[24] N. Arkani-Hamed, G.L. Kane, J. Thaler, L.T. Wang, J. High Energy Phys. 0608 (2006) 070. [hep-ph/0512190].
[25] J. Abdallah, A. Ashkenazi, A. Boveia, G. Busoni, A. De Simone, C. Doglioni, A. Efrati, E. Etzion, et al. arXiv:1409.2893 [hep-ph].
[26] S. Malik, C. McCabe, H. Araujo, A. Belyaev, C. Boehm, J. Brooke, O. Buchmueller, G. Davies, et al. arXiv:1409.4075 [hep-ex].
[27] L.J. Hall, L. Randall, Phys. Rev. Lett. 65 (1990) 2939.
[28] R.S. Chivukula, H. Georgi, Phys. Lett. B 188 (1987) 99.
[29] A.J. Buras, P. Gambino, M. Gorbahn, S. Jäger, L. Silvestrini, Phys. Lett. B 500 (2001) 161. [hep-ph/0007085].
[30] G. D'Ambrosio, G.F. Giudice, G. Isidori, A. Strumia, Nuclear Phys. B 645 (2002) 155. [hep-ph/0207036].
[31] M.J. Dolan, C. McCabe, F. Kahlhoefer, K. Schmidt-Hoberg, J. High Energy Phys. 1503 (2015) 171. arXiv:1412.5174 [hep-ph].
[32] R.C. Cotta, J.L. Hewett, M.P. Le, T.G. Rizzo, Phys. Rev. D 88 (2013) 116009. arXiv:1210.0525 [hep-ph].
[33] U. Haisch, A. Hibbs, E. Re, Phys. Rev. D 89 (2014) 034009. arXiv:1311.7131 [hep-ph].
[34] A. Crivellin, U. Haisch, A. Hibbs, Phys. Rev. D 91 (7) (2015) 074028. arXiv:1501.00907 [hep-ph].
[35] M. Abdullah, A. DiFranzo, A. Rajaraman, T.M.P. Tait, P. Tanedo, A.M. Wijangco, Phys. Rev. D 90 (2014) arXiv:1404.6528 [hep-ph].
[36] U. Haisch, F. Kahlhoefer, J. Unwin, J. High Energy Phys. 1307 (2013) 125. arXiv:1208.4605 [hep-ph].
[37] T. Lin, E.W. Kolb, L.T. Wang, Phys. Rev. D 88 (2013) 063510. arXiv:1303.6638 [hep-ph].
[38] P.J. Fox, C. Williams, Phys. Rev. D 87 (2013) 054030. arXiv:1211.6390 [hep-ph].
[39] M.R. Buckley, D. Feld, D. Goncalves, Phys. Rev. D 91 (1) (2015) arXiv:1410.6497 [hep-ph].
[40] P. Harris, V.V. Khoze, M. Spannowsky, C. Williams, Phys. Rev. D 91 (5) (2015) 055009. arXiv:1411.0535 [hep-ph].
[41] U. Haisch, E. Re, arXiv:1503.00691 [hep-ph].
[42] G. Artoni, T. Lin, B. Penning, G. Sciolla, A. Venturini, arXiv:1307.7834 [hep-ex].
[43] CMS Collaboration, http://cds.cern.ch/record/1697173/files/B2G-13-004-pas.pdf.
[44] CMS Collaboration, http://cds.cern.ch/record/1749153/files/B2G-14-004-pas.pdf.
[45] G. Aad, et al. [ATLAS Collaboration], arXiv:1410.4031 [hep-ex].
[46] U. Haisch, F. Kahlhoefer, E. Re, J. High Energy Phys. 1312 (2013) 007. arXiv:1310.4491 [hep-ph].
[47] R.M. Godbole, G. Mendiratta, T.M.P. Tait, arXiv:1506.01408 [hep-ph].
[48] J. Alwall, M. Herquet, F. Maltoni, O. Mattelaer, T. Stelzer, J. High Energy Phys. 1106 (2011) 128. arXiv:1106.0522 [hep-ph].
[49] C. Degrande, C. Duhr, B. Fuks, D. Grellscheid, O. Mattelaer, T. Reiter, Comput. Phys. Commun. 183 (2012) 1201. arXiv:1108.2040 [hep-ph].
[50] A. Abramowski, F. Acero, F. Aharonian, et al., High Energy Astrophysical Phenomena 750 (2012) 123. arXiv:1202.5494 [astro-ph].
[51] F. Aharonian, et al., [HESS Collaboration], Phys. Rev. D 78 (2008) 072008. arXiv:0806.2981 [astro-ph].
[52] M.A. Shifman, A.I. Vainshtein, V.I. Zakharov, Phys. Lett. B 78 (1978) 443.
[53] A. Crivellin, M. Hoferichter, M. Procura, Phys. Rev. D 89 (5) (2014) 054021. arXiv:1312.4951 [hep-ph].
[54] P. Junnarkar, A. Walker-Loud, Phys. Rev. D 87 (2013) 114510. arXiv:1301.1114 [hep-lat].
[55] C.P. Burgess, M. Pospelov, T. ter Veldhuis, Nuclear Phys. B 619 (2001) 709. [hep-ph/0011335].
[56] V. Barger, P. Langacker, M. McCaskey, M.J. Ramsey-Musolf, G. Shaughnessy, Phys. Rev. D 77 (2008) arXiv:0706.4311 [hep-ph].
[57] A. Djouadi, O. Lebedev, Y. Mambrini, J. Quevillon, Phys. Lett. B 709 (2012) 65. arXiv:1112.3299 [hep-ph].
[58] A. Djouadi, A. Falkowski, Y. Mambrini, J. Quevillon, Eur. Phys. J. C 73 (6) (2013) 2455. arXiv:1205.3169 [hep-ph].
[59] J.M. Cline, K. Kainulainen, P. Scott, C. Weniger, Phys. Rev. D 88 (2013) 055025. arXiv:1306.4710 [hep-ph].
[60] V.V. Khoze, C. McCabe, G. Ro, J. High Energy Phys. 1408 (2014) 026. arXiv:1403.4953 [hep-ph].
[61] N. Craig, H.K. Lou, M. McCullough, A. Thalapillil, arXiv:1412.0258 [hep-ph].
[62] Y.G. Kim, K.Y. Lee, S. Shin, J. High Energy Phys. 0805 (2008) 100. arXiv:0803.2932 [hep-ph].
[63] S. Baek, P. Ko, W.I. Park, J. High Energy Phys. 1202 (2012) 047. arXiv:1112.1847 [hep-ph].
[64] L. Lopez-Honorez, T. Schwetz, J. Zupan, Phys. Lett. B 716 (2012) 179. arXiv:1203.2064 [hep-ph].
[65] L. Carpenter, A. DiFranzo, M. Mulhearn, C. Shimmin, S. Tulin, D. Whiteson, Phys. Rev. D 89 (7) (2014) 075017. arXiv:1312.2592 [hep-ph].
[66] R. Enberg, P.J. Fox, L.J. Hall, A.Y. Papaioannou, M. Papucci, J. High Energy Phys. 0711 (2007) 014. arXiv:0706.0918 [hep-ph].
[67] R. Mahbubani, L. Senatore, Phys. Rev. D 73 (2006) [hep-ph/0510064].
[68] C. Cheung, D. Sanford, J. Cosmol. Astropart. Phys. 1402 (2014) 011. arXiv:1311.5896 [hep-ph].
[69] T. Cohen, J. Kearney, A. Pierce, D. Tucker-Smith, Phys. Rev. D 85 (2012) 075003. arXiv:1109.2604 [hep-ph].
[70] T. Hambye, A. Strumia, Phys. Rev. D 88 (2013) 055022. arXiv:1306.2329 [hep-ph].
[71] W. Altmannshofer, W.A. Bardeen, M. Bauer, M. Carena, J.D. Lykken, J. High Energy Phys. 1501 (2015) 032. arXiv:1408.3429 [hep-ph].
[72] S.R. Coleman, E.J. Weinberg, Phys. Rev. D 7 (1973) 1888.
[73] K.A. Meissner, H. Nicolai, Phys. Lett. B 648 (2007) 312. [hep-th/0612165].
[74] R. Foot, A. Kobakhidze, K.L. McDonald, R.R. Volkas, Phys. Rev. D 77 (2008) 035006. arXiv:0709.2750 [hep-ph].
[75] C. Englert, J. Jaeckel, V.V. Khoze, M. Spannowsky, J. High Energy Phys. 1304 (2013) 060. arXiv:1301.4224 [hep-ph].
[76] G. Aad, et al., [ATLAS Collaboration], Phys. Rev. Lett. 112 (2014) 201802. arXiv:1402.3244 [hep-ex].
[77] S. Chatrchyan, et al., [CMS Collaboration], Eur. Phys. J. C 74 (2014) 2980. arXiv:1404.1344 [hep-ex].
[78] A. Farzinnia, H.J. He, J. Ren, Phys. Lett. B 727 (2013) 141. arXiv:1308.0295 [hep-ph].
[79] G. Belanger, B. Dumont, U. Ellwanger, J.F. Gunion, S. Kraml, Phys. Lett. B 723 (2013) 340. arXiv:1302.5694 [hep-ph].
[80] A.A. Petrov, W. Shepherd, Phys. Lett. B 730 (2014) 178. arXiv:1311.1511 [hep-ph].
[81] L. Calibbi, A. Mariotti, P. Tziveloglou, arXiv:1505.03867 [hep-ph].
[82] [ALEPH and DELPHI and L3 and OPAL and SLD and LEP Electroweak Working Group and SLD Electroweak Group and SLD Heavy Flavour Group Collaborations], S. Schael, et al., Phys. Rep. 427 (2006) 257. [hep-ex/0509008].
[83] B. Holdom, Phys. Lett. B 166 (1986) 196.
[84] K.S. Babu, C.F. Kolda, J. March-Russell, Phys. Rev. D 57 (1998) 6788. [hep-ph/9710441].
[85] P.J. Fox, J. Liu, D. Tucker-Smith, N. Weiner, Phys. Rev. D 84 (2011) 115006. arXiv:1104.4127 [hep-ph].
[86] A. Alves, S. Profumo, F.S. Queiroz, J. High Energy Phys. 1404 (2014) 063. arXiv:1312.5281 [hep-ph].
[87] G. Arcadi, Y. Mambrini, M.H.G. Tytgat, B. Zaldivar, J. High Energy Phys. 1403 (2014) 134. arXiv:1401.0221 [hep-ph].
[88] O. Lebedev, Y. Mambrini, Phys. Lett. B 734 (2014) 350. arXiv:1403.4837 [hep-ph].
[89] C.D. Carone, H. Murayama, Phys. Rev. D 52 (1995) 484. [hep-ph/9501220].
[90] E.J. Chun, J.C. Park, S. Scopel, J. High Energy Phys. 1102 (2011) 100. arXiv:1011.3300 [hep-ph].
[91] M.T. Frandsen, F. Kahlhoefer, S. Sarkar, K. Schmidt-Hoberg, J. High Energy Phys. 1109 (2011) 128. arXiv:1107.2118 [hep-ph].
[92] K.A. Olive, et al., [Particle Data Group Collaboration], Chin. Phys. C 38 (2014).
[93] M. Duerr, P. Fileviez Perez, Phys. Lett. B 732 (2014) 101. arXiv:1309.3970 [hep-ph].
[94] M. Duerr, P. Fileviez Perez, Phys. Rev. D 91 (9) (2015) arXiv:1409.8165 [hep-ph].
[95] O. Buchmueller, M.J. Dolan, S.A. Malik, C. McCabe, J. High Energy Phys. 1501 (2015) 037. arXiv:1407.8257 [hep-ph].
[96] M. Fairbairn, J. Heal, Phys. Rev. D 90 (11) (2014) 115019. arXiv:1406.3288 [hep-ph].
[97] T. Jacques, K. Nordström, arXiv:1502.05721 [hep-ph].
[98] M. Chala, F. Kahlhoefer, M. McCullough, G. Nardini, K. Schmidt-Hoberg, arXiv:1503.05916 [hep-ph].
[99] H. An, R. Huo, L.T. Wang, Phys. Dark Univ. 2 (2013) 50. arXiv:1212.2221 [hep-ph].
[100] C.W. Chiang, T. Nomura, K. Yagyu, arXiv:1502.00855 [hep-ph].
[101] V. Khachatryan, et al. [CMS Collaboration]. arXiv:1411.2646 [hep-ex].
[102] M. de Vries, J. High Energy Phys. 1503 (2015) 095. arXiv:1409.4657 [hep-ph].
[103] S. Chang, R. Edezhath, J. Hutchinson, M. Luty, Phys. Rev. D 89 (1) (2014) 015011. arXiv:1307.8120 [hep-ph].
[104] Y. Bai, J. Berger, J. High Energy Phys. 1311 (2013) 171. arXiv:1308.0612 [hep-ph].
[105] N.F. Bell, J.B. Dent, A.J. Galea, T.D. Jacques, L.M. Krauss, T.J. Weiler, Phys. Rev. D 86 (2012) 096011. arXiv:1209.0231 [hep-ph].
[106] H. An, L.T. Wang, H. Zhang, Phys. Rev. D 89 (11) (2014) 115014. arXiv:1308.0592 [hep-ph].
[107] A. DiFranzo, K.I. Nagao, A. Rajaraman, T.M.P. Tait, J. High Energy Phys. 1311 (2013) 014. [JHEP 1401, 162 (2014)] arXiv:1308.2679 [hep-ph].
[108] M. Papucci, A. Vichi, K.M. Zurek, J. High Energy Phys. 1411 (2014) 024. arXiv:1402.2285 [hep-ph].
[109] P. Agrawal, S. Blanchet, Z. Chacko, C. Kilic, Phys. Rev. D 86 (2012) 055002. arXiv:1109.3516 [hep-ph].
[110] J. Kile, Modern Phys. Lett. A 28 (2013) 1330031. arXiv:1308.0584 [hep-ph].
[111] P. Agrawal, B. Batell, D. Hooper, T. Lin, Phys. Rev. D 90 (6) (2014) 063512. arXiv:1404.1373 [hep-ph].
[112] D. Alves, et al., [LHC New Physics Working Group Collaboration], J. Phys. G 39 (2012) 105005. arXiv:1105.2838 [hep-ph].
[113] A. Kumar, S. Tulin, Phys. Rev. D 87 (9) (2013) 095006. arXiv:1303.0332 [hep-ph].
[114] B. Batell, T. Lin, L.T. Wang, J. High Energy Phys. 1401 (2014) 075. arXiv:1309.4462 [hep-ph].
[115] C. Kilic, M.D. Klimek, J.H. Yu, Phys. Rev. D 91 (5) (2015) 054036. arXiv:1501.02202 [hep-ph].
[116] K. Griest, D. Seckel, Phys. Rev. D 43 (1991) 3191.
[117] J. Edsjo, P. Gondolo, Phys. Rev. D 56 (1997) 1879. [hep-ph/9704361].